JOURNAL OF
EMERGING
INVESTIGATORS
VOLUME 2, ISSUE 12 | DECEMBER 2019
emerginginvestigators.org

Anti-Alzheimer's plants

Neuroprotective therapies based on plant extracts

Anonymity and generosity

Going unnamed reduces teens' propensity to give

Vibrotactile prosthetics

Sensory feedback improves artifical limb accuracy

Herbal cancer treatment

This antioxidant compound reduces cancer cells' evasiveness

JOURNAL OF EMERGING INVESTIGATORS

The Journal of Emerging Investigators is an open-access journal that publishes original research in the biological and physical sciences that is written by middle and high school students. JEI provides students, under the guidance of a teacher or advisor, the opportunity to submit and gain feedback on original research and to publish their findings in a peer-reviewed scientific journal. Because grade-school students often lack access to formal research institutions, we expect that the work submitted by students may come from classroom-based projects, science fair projects, or other forms of mentor-supervised research.

JEI is a non-profit group run and operated by graduate students, postdoctoral fellows, and professors across the United States.

Contents

VOLUME 2, ISSUE 12 | DECEMBER 2019

JOURNAL OF
EMERGING INVESTIGATORS

Article

Potential multifunctional agents for dual therapy of age-related and associated diseases: Alzheimer's disease and Type 2 Diabetes Mellitus

Rohan Kumar and Leya Joykutty
American Heritage School, Plantation, Florida

SUMMARY

Currently there is no cure for Alzheimer's Disease (AD) and there seems to be an age-related link between AD and Type 2 Diabetes Mellitus (DM) in terms of incidence, symptoms and causation. The objective of this experiment is to assess the biological potentials of methanol extracts and its derived fractions of four Ayurvedic plants *Buchania axillaris*, *Hemidesmus indicus*, *Pavetta indica* and *Ochna obtusa* to develop potent agents for dual therapy of both AD and DM. Plant extracts in different concentrations were used in five colorimetric assays: Cholinesterase (AChE, BuChE inhibition) assay, Glucosidase (α–Glu) inhibition assay, an antioxidant activity assay, and MTT assay for cell viability and neuroprotective effects. It was found that that methanolic extract and its derived chloroform fraction of plants exhibited high inhibitory activity against AChE, BuChE, α–Glc enzymes. The active chloroform fractions also showed high antioxidant potential and neuroprotective capacity against H2O2 induced oxidative stress in human neuroblastoma cells. In all the assays, the samples were statistically different than the negative control meaning that the samples with the plant extracts were more effective than the controls without the treatment, while being as effective as the positive controls, which included current drugs used to treat the diseases individually.

INTRODUCTION

Type 2 Diabetes Mellitus (DM) is an age-related metabolic disorder with complex etiology and affects 10% of the population across the world (1). Currently there are 366 million people with DM worldwide, and this is expected to worsen in the next 20 years and reach 552 million by 2030 (2). DM is characterized by cellular insulin resistance, chronic inflammation, and several metabolic abnormalities. It often leads to macro- and micro-vascular complications that accelerate aging and can damage several organ systems (3).

Alzheimer's disease (AD) is the most common form of dementia, accounting for 60–80% of all dementia cases (4). AD is an irreversible, progressive brain disorder that slowly destroys memory and thinking skills. AD affects 46.8 million people worldwide and this number is likely to double by 2030 due to lack of an effective cure (5). Many abnormal clumps (called amyloid beta (Aβ) plaques) and tangled bundles of fibers (called neurofibrillary, or tau, tangles) are characteristics of Alzheimer patients' brains (5). While it remains unknown exactly what role plaques and tangles play in AD, it is believed that they somehow play a critical role in blocking communication among nerve cells and disrupting processes that cells need to survive (4). This destruction of nerve cells causes memory failure, personality changes, problems carrying out daily activities, and other symptoms characteristic of AD (6).

According to many reports, DM is considered to be a chief risk factor for AD as it increases the incidence by almost two-fold (3). Early accumulation of Aβ is partially responsible for central nervous system insulin resistance and impaired insulin signaling. This leads to the onset of both diseases as it initiates brain injury via inflammatory and oxidative stress processes (3) (**Figure 1**).

The chronic elevation of serum glucose in DM is called hyperglycemia. Therapies designed to reverse the chronic hyperglycemia in DM in a noninvasive manner are mostly based on inhibition of intestinal absorption of sugar (7). Before carbohydrates are absorbed from food, they must be broken down into smaller sugar particles like glucose by enzymes in the small intestine. One of the enzymes involved in breaking down carbohydrates is called alpha glucosidase (*α*-Glu). One of the therapeutic approaches to decrease postprandial hyperglycemia is the inhibition of carbohydrate hydrolyzing enzymes such as α–glucosidases (α–Glu), thereby delaying glucose digestion in the digestive tract. Alpha-glucosidase inhibitors thus may be able to prevent the development of diabetic symptoms (2).

Acetylcholinesterase also known as AChE or acetylhydrolase, is an enzyme that catalyzes the breakdown of acetylcholine (ACh), an important neurotransmitter. AChE is found mainly at neuromuscular junctions and in chemical synapses where it serves to terminate synaptic transmission by hydrolyzing ACh (8).

Low levels of ACh are considered to play definitive roles in the pathophysiology of AD due to their dramatic effect on the cholinergic system. (9). According to the "cholinergic

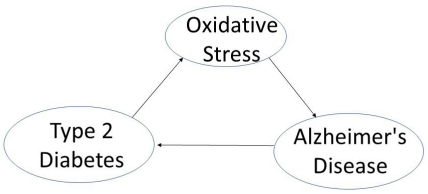

Figure 1: The Diabetes-Alzheimer's Cylce. Diabetes Mellitus(DM) is a risk factor for Alzheimer's DIsease, while amyloid beta plaques characteristic of AD increases insulin resistince leading to DM as well as oxidative stress leading to brain injury.

hypothesis", AChE acts primarily as a regulatory enzyme at cholinergic synapses (9), while butyrylcholinesterase (BuChE), an enzyme closely related to AChE, serves as a co-regulator of cholinergic neurotransmission by hydrolyzing ACh (10). Concerning the cholinergic hypothesis, one rational and effective approach to treat AD's symptoms is raising the ACh through inhibition of AChE, which is responsible for hydrolysis of ACh. Furthermore, BuChE, the second member of the cholinesterase family, seems to be involved in the hydrolysis of ACh during the last stages of the disease to compensate for the reduced levels of AChE (10). Moreover, AChE and BuChE are responsible for upregulating the expression of the amyloid precursor protein (APP) (10). Therefore, dual inhibition of AChE and BuChE could be effective in the management of AD symptoms.

Oxidative stress is one of the earliest events in the pathogenesis of both AD and DM (7). Oxidative stress is defined as the imbalance between the generation of reactive oxygen/nitrogen species (ROS/RNS) and the cell's ability to neutralize them by the antioxidant defense. The ROS/RNS are capable of damaging and modifying several types of macromolecules within the cell, including DNA, RNA, lipids, and proteins. Oxidation of lipids could be deleterious since this has the potential to damage the cell membranes. Numerous studies have also suggested that oxidative stress and A*β* protein are linked to each other (11). Therefore, the antioxidants that scavenge free radicals have proven to be a treatment option for AD and T2D (11).

Medicinal plants have always been recognized as an important source of secondary metabolites with various beneficial effects on human health. They are regarded as valuable material for the development of modern medicines, nutraceuticals, food supplements, pharmaceutical intermediates, and chemical entities for synthetic drugs. However, due to less effort towards examining extracts of plants, scientific information on medicinal properties of various plants is still scarce. Ayurveda is an ancient Indian medicinal system practiced from 2000 BC in which plants with medicinal properties are well documented (12). Based on traditional anti-inflammatory and antioxidant uses in Ayurveda (13), the following plants were selected for the study: *Buchania axillaris* (BA) (14), *Hemidesmus indicus* (HI) (15-17), *Pavetta indica* (PI) (18-19), and *Ochna obtusata* (OO) (20-21). Methanolic extractions of the above plants (BAM, HIM, PIM, OOM) and fractionations in water (BAW, HIW, PIW, OOW) and chloroform (BAC, HIC, PIC, OOC) of the above plants were used in the experiment.

The objective of the experiment was to explore an *in vitro* multipronged treatment option for both DM and AD that could be cost effective with minimal side effects. It was hypothesized that the methanolic extracts and fractionations of test plants (BA, HI, PI, OO) would show concentration dependent inhibitory activities against AChE, BuChE enzymes, α–glucosidase enzymes while providing antioxidant and neuroprotective benefits. This experiment assessed the biological potentials including anticholinesterase, α–Glucosidase inhibition, antioxidant, and neuroprotective activity of methanol extracts and its derived fractions of *B. axillaris* , *H.indicus*, *P. indica* , and *O.obtusa* to develop potent agents for dual therapy of both AD and DM.

RESULTS

In order to evaluate the plant extracts for their multifunctional potency against both Alzheimer's Disease and Type 2 Diabetes, several invitro assays on relevant targets of AD and DM have been used. The methanolic extract and its derived chloroform fraction of the four plants screened (BA, HI, PI, OO) exhibited satisfactory inhibitory activity against AChE, BuChE, α–Glc enzymes. They also showed high antioxidant potential and neuroprotective capacity against H2O2 induced oxidative stress in neuronal cells.

The Effect of Plant Extracts on AChE and BuChE Inhibition

The methanolic extracts of four plants and their derived fractions were screened for their inhibitory activity against AChE and BuChE enzymes using Ellman's colorimetric method (22). The cholinesterase Assay is based on an improved Ellman method, in which thiocholine produced by the action of AChE and BuChE forms a yellow color with 5,5'-dithiobis(2-nitrobenzoic acid). The intensity of the product color, measured at 412 nm, is proportionate to the enzyme activity in the sample.

All the plant extracts and fractions evaluated at different concentrations (60, 90, and 150 µg/mL) showed dose-dependent inhibitory activities against enzymes AChE and BuChE. Galantamine (brand names Razadyne, Reminyl, and others) is used for the treatment of cognitive decline in mild to moderate Alzheimer's disease and various other memory impairments and is known for its acetylcholinesterase (AChE)-inhibiting properties and was thus used as the positive control

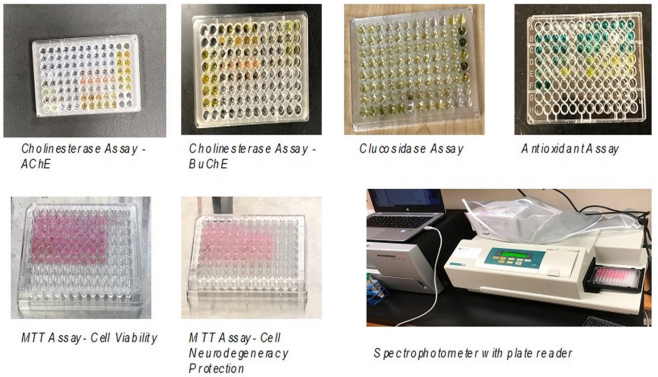

Figure 2. Spectrophotometer and Colorimetry. Most spectrophotoreaders apply a logarithmic function to the linear transmittance ratio to calculate the "absorbance" of the sample. This is proportional to the concentration of the chemical being measured. In the experiments conducted, there is an inverse relationship between the effectiveness of the extracts and the density reading (indicated by the lighter color) and a direct relationship between enzyme activity and the readings.

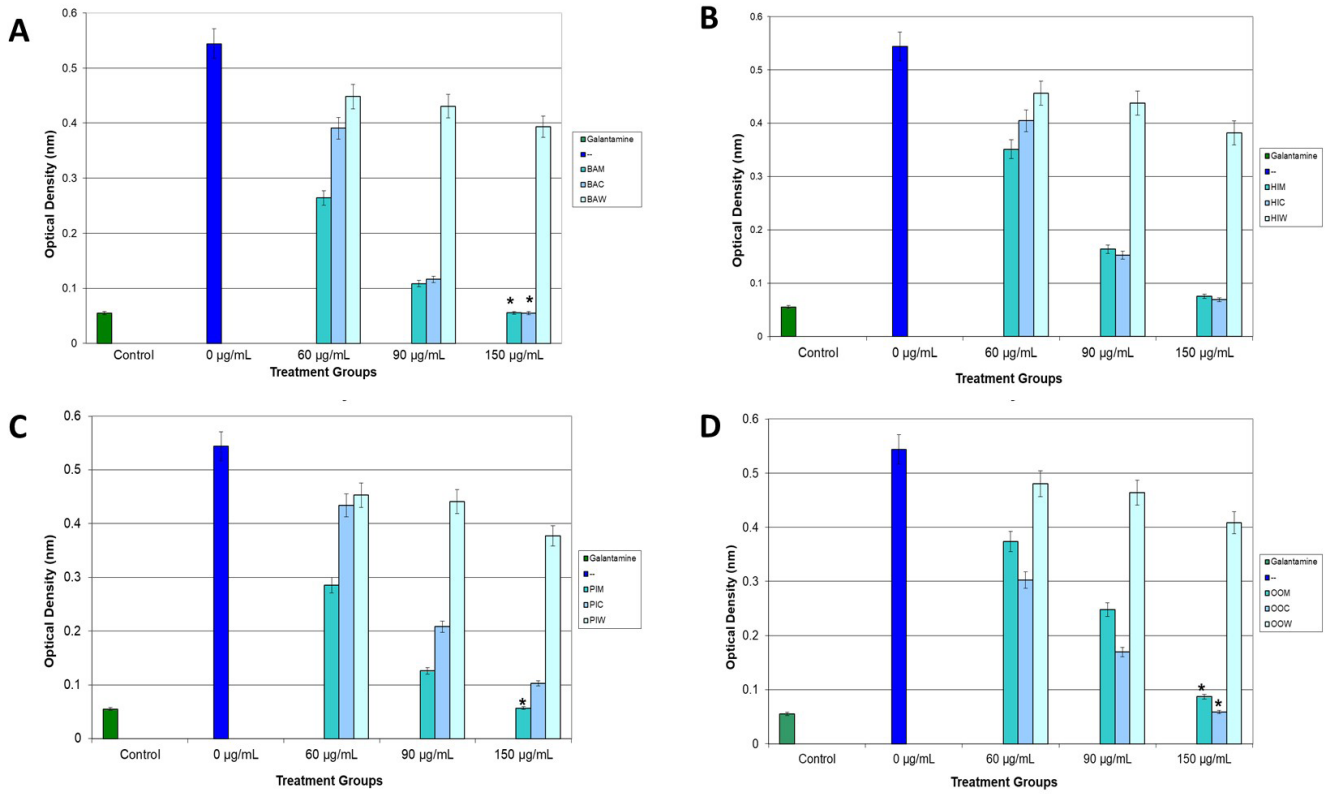

Figure 3. AChE inhibition by the plant extracts. Mean spectrophotometer readings for A. *B. axillaris* B. *H. indicus*, C. *P. indica* D. *O. obtusa* (Data are mean +/- SD (n=3) and asterisk indicate that there was no significant difference between the treatment and the Control at 95% confidence)

drug. The lower the spectrophotometer reading, the higher the inhibitory activity (the color developed due to the formation of the 5-thio-2-nitrobenzoate anion, indicating the inhibition activity—the lighter the color, the greater the inhibition of the enzyme). (**Figure 2**). BAM, HIM, and PIM extracts were potent in inhibiting AChE and BuChE enzymes (**Figures 3 & 4**). Among the fractions, BAC, HIC, and OOC showed higher activity than other fractions against AChE and BuChE enzymes. In the case of water fractions, only HIW displayed moderate activity against both AChE and BuChE. Overall, the most prominent AChE inhibition was recorded with BA, while HI was most active against BuChE. All plants showed reduced activity against AChE when compared to galantamine. Of the fractions, BAC, HIC, OOC, PIC, and PIW showed moderate inhibition on AChE activity (Figure 3). However, BAM, HIM, and HIC exhibited stronger inhibition against BuChE. BAC, HIC, HIW, PIC, and OOC showed significant inhibition on BuChE activity (student's t -test $p<0.05$) (**Figure 4**).

The Effect of Plant Extracts on α-Glucosidase Inhibition

As mentioned earlier, α-Glucosidase decomposes disaccharides into glucose, and increases blood glucose levels. Therefore, an increase in blood glucose can be suppressed by inhibiting the activity of α-Glucosidase (**Figure 5**). To assess the antidiabetic potency of the plants, the extracts and derived fractions were tested for their α–Glucosidase inhibitory activity by invitro enzyme assay. In this assay α-Glucosidase hydrolyzes the substrate mix to release the *p*-nitrophenol that can be measured colorimetrically (OD = 410 nm). Enzyme activity was measured by the quantity of *p*-nitrophenol released. The lower the quantity of *p*-nitrophenol released, the higher the inhibitory action against the glucosidase enzyme and higher the absorbance (**Figure 2**). All the plant extracts and fractions showed dose-dependent inhibitory action against *α*–Glucosidase when compared to the sample without the extracts (**Figure 6**). Acarbose, a drug commonly used to lower blood sugar in patients with high blood sugar, was used as the positive control drug. All the plants displayed greater inhibition of α–Glucosidase than the positive control drug acarbose with BAC, HIM, HIC, PIC, and OOC being the most active, HIW and PIW were moderately active, and BAW was the least active against the enzyme.

Radical Scavenging Activity of the Plant Extracts

The ABTS (2,2'-azinobis-(3-ethylbenzothiazoline-6-sulfonate)) assay is a widely accepted antioxidant assay to screen the total antioxidant power of fruits, vegetables, foods, and plants. In particular, it is recommended to be used for plant extracts because the long wavelength absorption maximum at 745 nm eliminates color interference in plant extracts. In this assay, the ABTS radical cation is generated by the oxidation of ABTS with potassium persulfate. Its reduction in

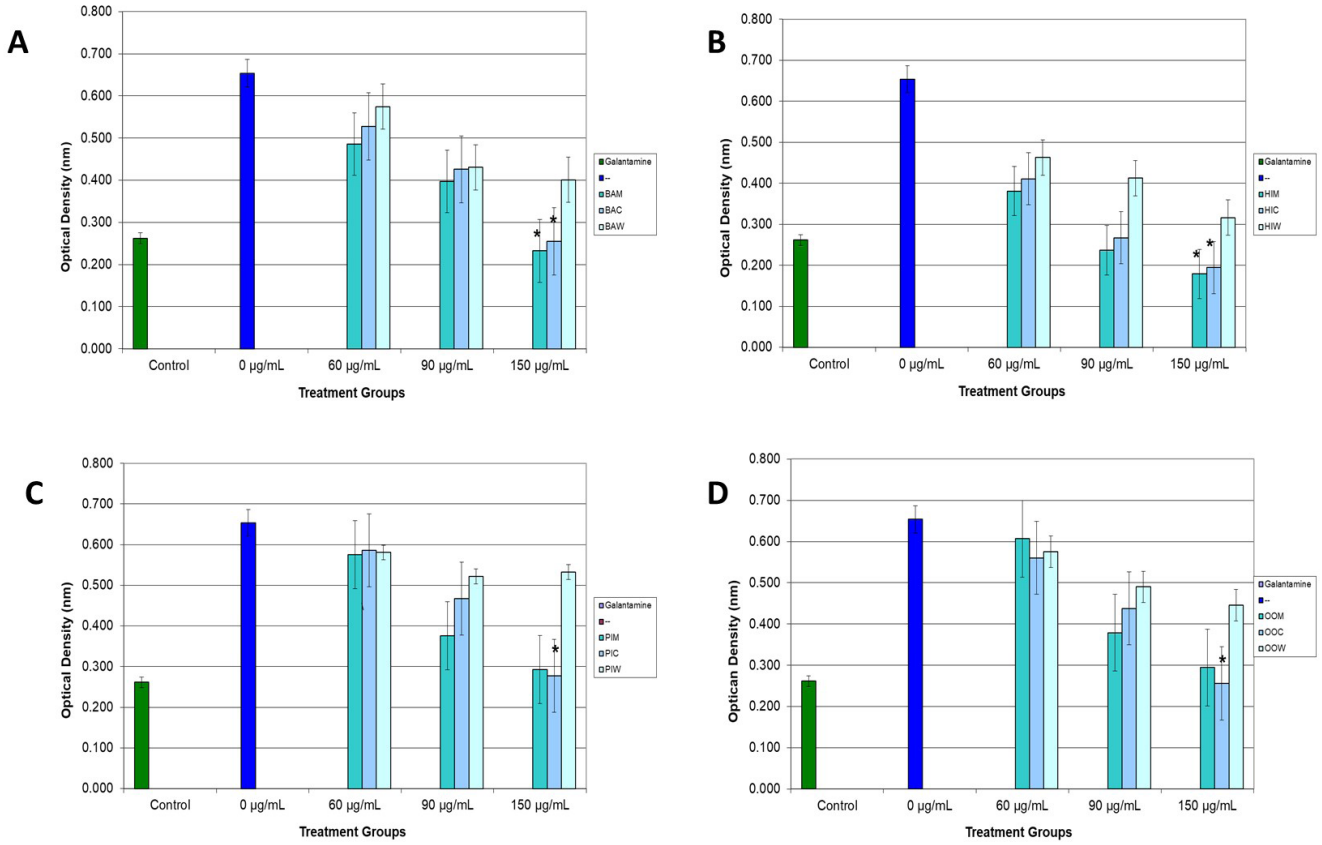

Figure 4. BuChE inhibition by the plant extracts. Mean spectrophotometer readings for A. *B. axillaris* B. *H. indicus,* C. *P. indica* D. *O. obtusa* (Data are mean +/- SD (n=3) and asterisk indicate that there was no significant difference between the treatment and the Control at 95% confidence)

the presence of hydrogen-donating antioxidants in chloroform fractions is measured spectrophotometrically. Trolox, a cell-permeable, water-soluble analogue of vitamin E, is used as a standard for measuring the antioxidant capacity of complex mixtures and is commonly used in biological or biochemical applications to reduce oxidative stress or damage. All the four plant extracts in the highest concentration in chloroform fractions had increased radical scavenging activity (RSA) compared to the control (Trolox), with the HIC and BAC being significantly effective (**Figure 7**).

Viability of Cells Treated with Extracts

The safety of the extract is absolutely crucial for a successful pharmaceutical formulation. In line with this, the possible toxic effects of active fractions BAC, HIC, PIC, and OOC in the human neuroblastoma SK-N-SH cells have been assayed with MTT assay. Neuroblastoma (NB) cell lines are transformed, neural crest-derived cells, capable of unlimited proliferation *in vitro*. These cell lines retain the ability of differentiation into neuronal cell types on treatment with various agents. This ability of NB cells to proliferate as well as to differentiate makes it an excellent *in vitro* system for various studies. NB cells are extensively used for testing neurotoxicity of putative drugs such as antimalarial or anticancer agents. They have been used to dissect the relationships between proliferation, differentiation and apoptosis. This feature has been useful in understanding the pediatric cancer--neuroblastoma and for development of

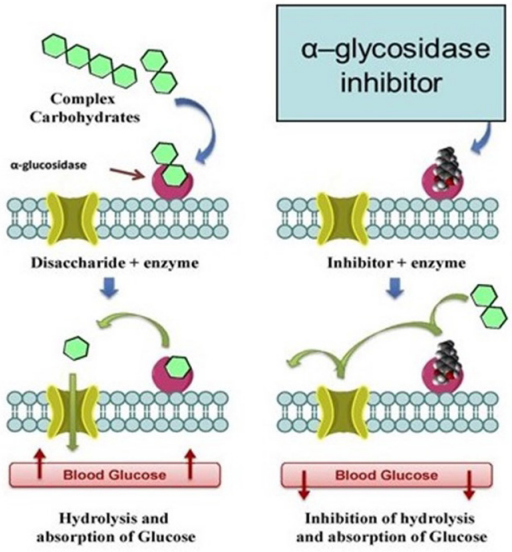

Figure 5: Plant extracts and hyperglycemia. Plant extracts can help with hyperglycemia by inhibiting carbohydrate hydrolyzing enzymes, in this case α–Glu (Picture courtesy: www.slideshare.net/featured/category/health-medicine)

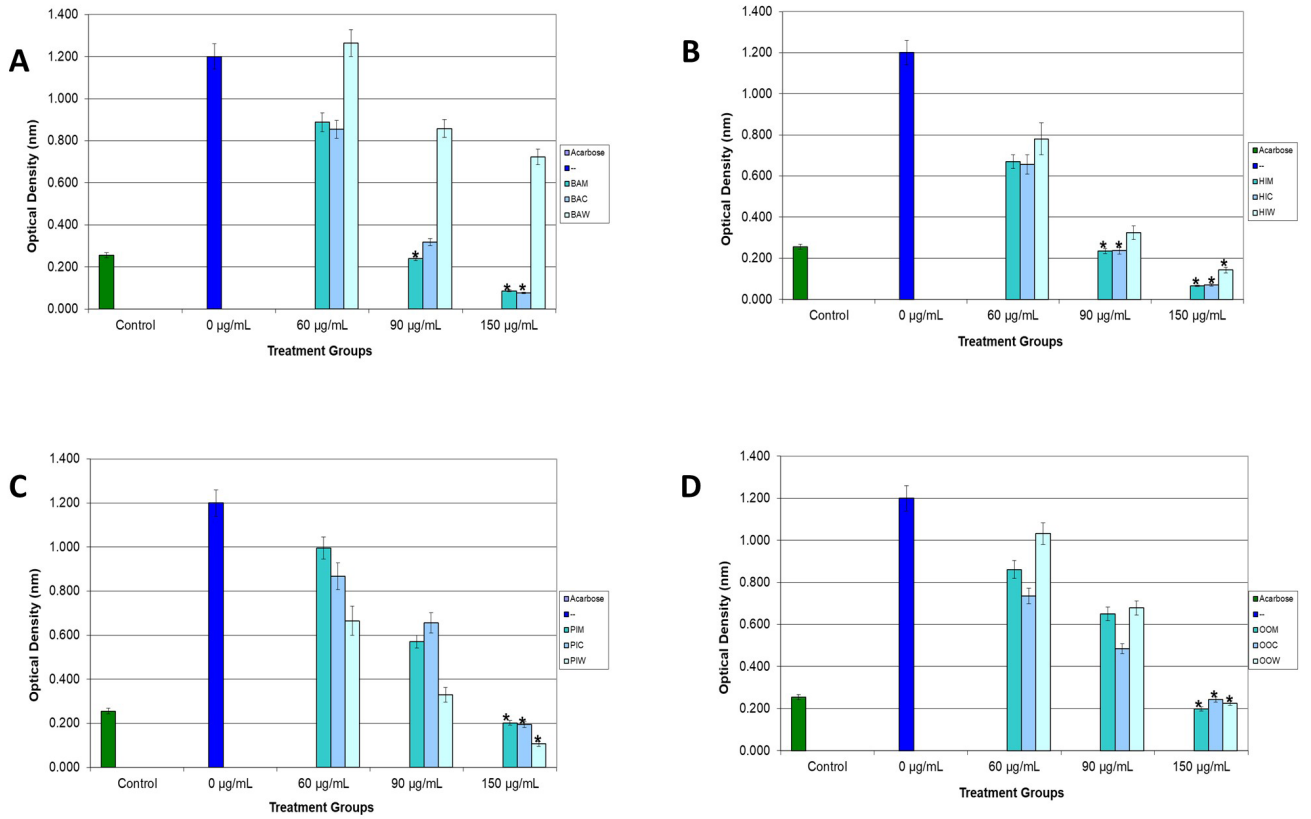

Figure 6. α–Glucosidase inhibition by the plant extracts: Mean spectrophotometer readings for A. *B. axillaris* B. *H. indicus*, C. *P. indica* D. *O. obtusa* (Data are mean +/- SD (n=3) and asterisk indicate that there was no significant difference between the treatment and the Control at 95% confidence)

newer therapies. Since currently, we cannot look at amyloid plaques and tangles until autopsy, studying the effect of the extracts on the cells is a good starting point

We measured the percentage of viable cells in the presence or absence (control) of several concentration of *B.axillaris*, *H.indicus* , *P. indica*, and *O. obtusata*. All the extract concentrations were not significantly different than the control cells at 95% confidence level (**Figure 8**). Under the experimental conditions, BAC, HIC, PIC, and OOC, displayed increased cell viability in a concentration-dependent manner. Among the tested fractions, fraction OOC attenuated the cell toxicity significantly in a concentration-dependent manner.

Neuroprotective Capacities against H_2O_2-Induced Cell Death in SK-N-SH Cells

The neuroprotective effect of selected plant fractions against H_2O_2-induced oxidative injury in SK-N-SH cells was determined by pretreating the cells with different concentrations of plant extract for three hours before treatment with H_2O_2. 1 mM H_2O_2 was added to induce oxidative stress in the cells (**Figure 9**) and the cell viability was measured by MTT colorimetry. The viability of SK-N-SH cells pretreated with 100, 200, or 400 µg of active fractions from BAC, HIC, PIC, and OOC for 24 hours before exposure to H_2O_2 was significantly increased relative to control in a dose-dependent manner (**Figure 10**). When the neuroprotective effect induced by fractions was compared with control (medium plus H_2O_2) the fraction HIC showed higher neuroprotectivity than the control at all concentrations. In fact, cells in the HIC fraction behaved almost similarly as the cells in medium only not exposed to H_2O_2. Fractions BAC, PIC, and OOC provided a higher neuroprotective profile to that of control at higher concentrations. This observation suggests that certain compounds present in fractions likely promoted cell survival or delayed the death of neurons when exposed to oxidative stress. Based on the results obtained, these fractions can be

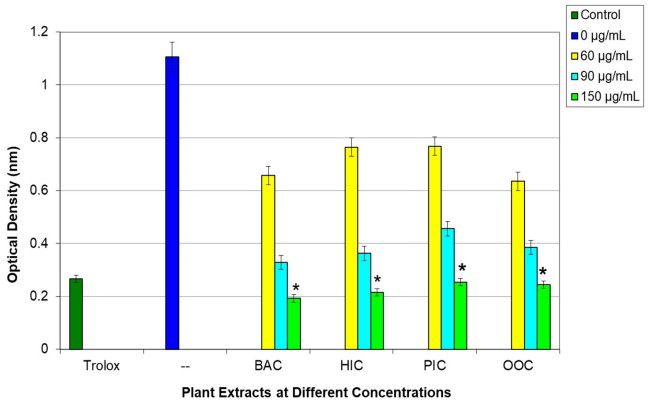

Figure 7. Radical scavenging activity of plant extracts. Data are mean spectrophotometric reafings +/- SD (n=3) and asterisk indicate that there was no significant difference between the treatment and the Control at 95% confidence.

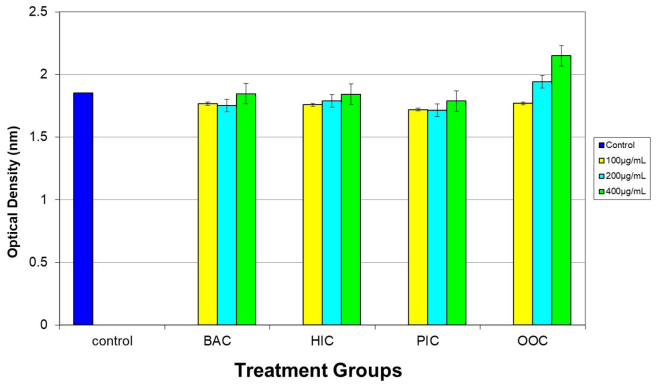

Figure 8. Figure 8: Cell viabilty of plant extract treated cells. Data are mean spectrophotometer readings +/- SD (n=3) and asterisk indicate that there was no significant difference between the treatment and the Control at 95% confidence.

considered as potential oxidative suppressors.

In conclusion, the present study demonstrates the *in vitro* potential of *B. axillaris, H. indicus, P. indica, and O. obtusata* as multifunctional therapeutic remedies for the treatment of AD and DM.

DISCUSSION

The objective of this experiment was to assess the biological potential of methanol extracts and the derived fractions of *B. axillaris* (BA), *H. indicus* (HI), *P. indica* (PI), and *O. obtusa* (OO) to help with both DM and AD with minimal side effects. This experiment was an attempt to use plants that were suggested to have some medicinal properties to combat age-related problems, like diabetes and Alzheimer's, by targeting the three areas of concern: high blood sugar, the depletion of ACh, and oxidative stress. In this study, the crude methanolic extracts of the plants were fractionated using polar and non-polar solvents to obtain phytoconstituent rich biologically active fractions. Methanol is commonly used for extraction of bioactive compounds as methanol is an amphiphilic compound and has a polarity index of 5:1. This means that methanol is widely used, mainly because many plant compounds dissolve in it with great freedom. It also easily evaporates so it can be separated from the extract. But for compounds that are strictly hydrophobic, a mixture of methanol and chloroform, or chloroform alone, was used for extraction of bioactive compounds. Subsequently, biological evaluations of extracts and fractions against various targets related to AD and DM suggest BA, HI, PI, and OO could serve as multifunctional agents for dual therapy.

Upholding ACh levels by reducing its metabolism in the synaptic cleft by inhibition of ChEs is beneficial for improvement in memory and cognitive dysfunction. Therefore, dual inhibition of AChE and BuChE of cholinergic neurotransmission is continuously referred to as the "gold standard" therapeutic strategy for the management of AD (10). The superior dual inhibitory potential of BAC, HIC, PIC, and OOC on AChE and BuChE in Cholinesterase assay indicates

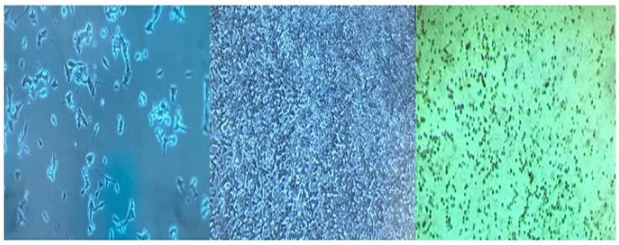

Figure 9. H_2O_2 induced oxidative stress on cells. Photographs of SK N SH cells in culture. Left panel is initial culture, middle panel is cells at 80% confluence, right panel is cells after H_2O_2 induced cell injury.

their potential as an alternative for the treatment of AD (**Figure 11**). Inhibition of α-glucosidase enzymes, which in turn delay in the digestion of carbohydrates, is an effective approach for the management of carbohydrate metabolic disorders like DM. Due to the strong inhibition of α-glucosidases, it is evident that the methanolic extracts and fractions BAC, HIC, PIC, and OOC have excellent antidiabetic potency.

Currently, the multifactorial biological pathways involved in AD and DM seem to share oxidative stress as a unifying factor. Oxidative stress may be either due to excessive production of ROS, loss of antioxidant defenses, or both. Consequently, scavenging of ROS has become highly beneficial and a promising strategy for the treatment of AD and DM. Presently, the increased activity against ABTS by the fractions BAC, HIC, PIC, and OOC show that the tested fractions have the capacity to prevent the potential damage by ROS (**Figure 11**).

The safety of the extract is absolutely crucial for a successful drug. Therefore, the possible toxicity effects of the active fractions of the four plants in the SK-N-SH cells were measured. Interestingly, in the cell viability assay, the escalating cell proliferation at even high concentrations suggested that fractions are nontoxic to SK-N SH-cells and likelypromote cell survival or delay the natural death of neurons in culture medium. (**Figure 8**) As fractions provided higher or almost similar neuroprotective profile to that of control at higher concentrations, BAC, HIC, PIC, and especially OOC, are considered to act as potential oxidative suppressors against H_2O_2-induced oxidative stress in SK-N-

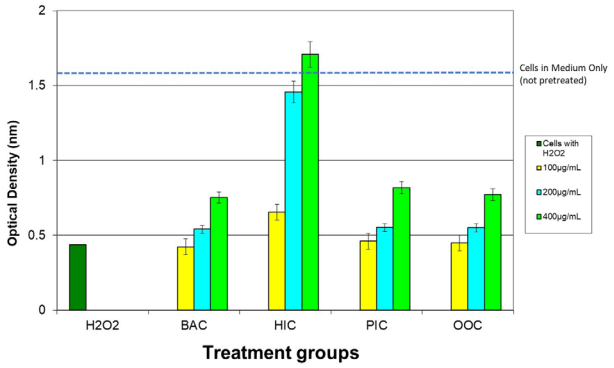

Figure 10. Spectrophotometer readings for Cell Neurodegeneracy. (Data are mean +/- SD (n=3))

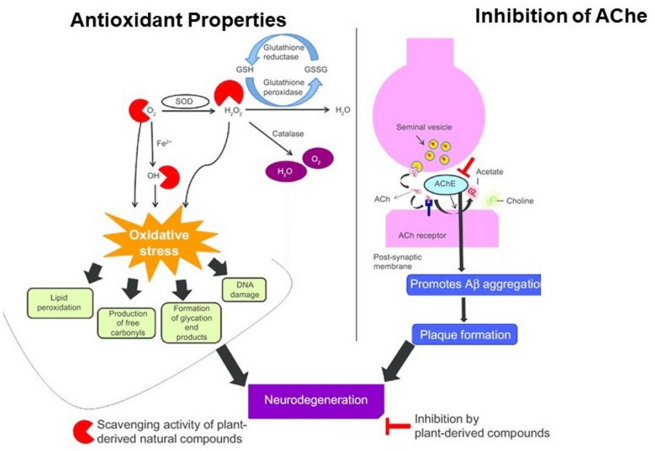

Figure 11. How plant extracts can help with AD. The plant extracts would help prevent degeneration by inhibiting AChE leading to increased levels of Ach while also scavenge for free radicals reducing oxidative stress (31)

SH cells (**Figure 10**).

Currently there is no cure for Alzheimer's Disease. The few agents approved by the US Federal Drug Administration for the treatment of AD and DM have less potency and multiple side effects (23). Consequently, it has become a necessity to develop the new agents that are pharmacologically safe, cost-effective, and immediately available with minimal side effects. The World Health Organization has also recommended the development of improved and safer herbal medicines (24). The findings of this experiment serve as a promising starting point for studying the therapeutic potential of these natural agents to break the DM and Alzheimer's cycle. However, because responses observed *in vitro* can be magnified, diminished, or totally different in more complex integrated systems, *in vivo* work is vital for the analysis of drug action and development of new therapeutic agents. Future *in vivo* research, such as experiments using a mouse model, needs to be conducted to see how the plant extracts react in a living organism, in precise cellular conditions.

METHODS

Plant Extracts

Plant samples were taken, dried, and ground to a powder and stored in a cool, dark place.

Ground plant material (100 g) was extracted with 500 ml of 90% methanol by soaking for two days and then filtered through Whatman No.1 filter paper. For this experiment, the crude methanolic extracts (20 g) were also suspended in water (50 mL) and chloroform (100 mL) was added and shaken well, and the layers were allowed to separate for 6 hours in a separating funnel. The remaining methanolic extracts were dried for three days in an oven. Chloroform and water layers were then separated and evaporated to obtain the chloroform fraction and water fractions. All the extracts were stored in a cool, dark place until ready for use.

Cholinesterase Enzyme Inhibition Assay (Methanolic and Chloroform Extracts)

Acetylcholinesterase (AChE) from *Electrophorus electricus* (electric eel) and Butyrylcholinesterase (BuChE) from equine serum were used in this assay. 10.85 mg of Acetylthiocholine iodide and Butyrylthiocholine iodide were mixed separately in 5 ml of Phosphate buffer (Substrate). 3.96 mg of Ellman's Reagent also known as DTNB (5,5'-dithio-bis-[2-nitrobenzoic acid]) and 1.5 mg of sodium bicarbonate were mixed to make DTNB solution. In a 96-well plate, 10 µL of enzyme (AChE, 2 U/mL or BuChE, 2 U/mL), 10 µL of plant extract/fraction (30, 90, 150 µg/mL), 100 µL of phosphate buffer, and 50 µL of DTNB solution were added. As an additional control, 150 µg/mL of galantamine was used. For a negative control, the test mixture without the plant samples was used. Three wells were used for each test sample (3 replicates for each methanolic, chloroform, and water fractions for each plant) and control. The plate was incubated for 5 minutes at 25ºC. 15 µL of the substrate was added, and the plate was incubated for another 5 minutes at 25ºC**.** A spectrophotometer reading at 412 nm was taken.

α-Glucosidase Inhibitory Assay (Methanolic and Chloroform Fractions)

In a 96-well plate, 50 µL of enzyme α-glucosidase (0.15 unit/mL), 10 µL of plant extract/fraction (30, 90, 150 µg/mL), and100 µL of phosphate buffer were added. For positive control, 150 µg/mL of Acarbose was used and for negative control. The test mixture without the plant samples was used. Three wells were made for each test sample (3 replicates for each methanolic, chloroform, and water fractions for each plant) and the control. The well was incubated for 15 minutes at 37ºC. 50 µL of the substrate 4-Nitrophenylα-D-glucopyranoside was added, and the plate was incubated further at 37ºC for 15 minutes. 50 µL of sodium bicarbonate was added to terminate the reaction. A spectrophotometer reading at 415 nm was taken to measure enzyme activity.

Antioxidant Activity Assay (Chloroform Fractions)

In a 96-well plate, 10 µL of Metmyoglobin(1 mg/mL), 10 µL of plant fraction (30, 90, 150 µg/mL), and 150 µL of Chromogen were added. For the positive control, 150 µg/mL of Trolox (a water-soluble analog of vitamin E) was used and for the negative control, the test mixture without the plant samples was used. Only chloroform fractions were used for this assay as the methanol could have an adverse reaction with the chemicals used for the assay. Three wells were used for each test sample (3 replicates for chloroform fraction for each plant) and the control. Different concentrations of Trolox (45, 90, 135, 180, 225 µg/mL) for the Trolox standard were prepared. The reaction was initiated by adding 40 µL of hydrogen peroxide (final concentration in the assay is 250µM) as quickly as possible, and the plate was incubated on shaker for 5 minutes at room temperature. Absorbance at 405 nm was read using a plate reader.

Cell Culture

SK-N-SH cells were cultured in MEM supplemented with 10% FBS and maintained at 37ºC in a humidified 5% carbon dioxide incubator. Cells were passaged every 4 days to get 6 flasks. When the cells reached 80% confluence, they were counted. Only plant extracts in chloroform fractions were used in the cell assays as methanol would react adversely with the cells.

Cell Viability Assay

Cytotoxic effects of selected plant fractions on the cell viability were measured using MTT assay. SK-N-SH cells were counted using a hemocytometer and cells (2×10^5 cells per well) in 200 mL of corresponding medium with 10% FBS were seeded into 96-wellplate. 1 µL of cells was added per well. Medium was removed and replaced with 100 µL of fresh medium along with plant fractions in chloroform at various concentrations (50, 100, 200, 400 µg/mL). 10 µL of the MTT labeling reagent was added to each well, including the ones with medium alone for a negative control. The microplate was incubated at 37ºC for 4 hours in a humidified incubator. 100 µL of Formazan solubilization solution was added to each well and mixed thoroughly, and the plate was incubated for 24 hours at 37ºC in a humidified incubator. The spectrophotometrical absorbance of the samples were measured at 570 nm.

Protection against Hydrogen Peroxide induced Cell Death Assay

1 µL of cells was added per well. Medium was removed and replaced with 100 µL of fresh medium along with plant fractions in chloroform at various concentrations (50, 100, 200, 400µg/mL). 10 µL of the MTT labeling reagent was added to each well, including the ones with medium alone for negative control. The microplate was incubated at 37ºC for 4 hours in a humidified incubator.

To induce oxidative stress, 1 mM of hydrogen peroxide was added to each well. (**Figure 3**). 100 µL of Formazan solubilization solution was added to each well and mixed thoroughly. The plate was incubated for 36 hours at 37ºC in a humidified incubator. The spectrophotometer absorbance of the samples was measured at 570 nm.

Equipment used

A spectrophotometer is able to determine what substances are present in a target and exactly how much through calculations of observed wavelengths. Colorimetry was used as a principle means of measuring the effectiveness of the extracts. Most spectrophotometers apply a logarithmic function to the linear transmittance ratio to calculate the absorbency of the sample, a value which is proportional to the concentration of the chemical being measured. The higher optical density readings indicated higher enzyme activity. In the cholinesterase and glucosidase assays, the effectiveness of the plant extracts in inhibiting enzyme activity was indicated by lower spectrophotometer readings. For the cell assays, the lighter the color, the less proliferation/viability of the cells (**Figure 11**).

Statistical Analysis

A student's t-test was used to determine if two sets of data are significantly different from each other. The null hypothesis tested here is that the experimental mean and the control mean are identical. Statistical hypothesis testing was performed by student's t-test and the values were considered as statistically significant when *p*-values were less than 0.05.

Received:
Accepted:
Published:

REFERENCES

1. Wi, W.L., *et al*. "Natural medicines used in the traditional Chinese medical system for therapy of diabetes mellitus." *Journal of Ethnopharmacology*, vol. 92, no. 1, 2004, pp. 1-21.
2. "Report on Diabetes." *World Health Organization, Geneva*, 2016, www.who.int/mediacentre/factsheets/fs312/en/.
3. Verdile, Giuseppe., *et al*. "The role of type 2 diabetes in neurodegeneration." *Neurobiology of Disease*, vol. 84, 2015, pp. 22-38.
4. "What Is Alzheimer's?- Alzheimer's Disease and Dementia." *alz.org*, www.alz.org/alzheimers-dementia/what-is-alzheimers.
5. "Alzheimer's Disease Fact Sheet." *National Institute on Aging*, www.nia.nih.gov/health/alzheimers-disease-fact-sheet.
6. Prince, Martin, *et al*. "The global prevalence of dementia: A systematic review and metaanalysis." *Alzheimer's and Dementia- The Journal of the Alzheimer's Association*., vol. 9, no. 1, 2013, pp. 63-75.
7. Butterfield, Allan, *et al*. "Elevated risk of type 2 diabetes for development of Alzheimer disease: A key role for oxidative stress in brain." *Biochimica et Biophysica Acta (BBA) - Molecular Basis of Disease*, vol. 1842, no. 9, 2014, pp. 1693-706.
8. Nyenwe, Ebenezer A *et al*. "Management of type 2 diabetes: evolving strategies for the treatment of patients with type 2 diabetes." *Metabolism: clinical and experimental* vol. 60, no.1, 2011, pp. 1-23. doi:10.1016/j.metabol.2010.09.010
9. Citron, Martin. "Alzheimer's disease: Strategies for disease modification." *Nature Reviews Drug Discovery*, vol. 9, no. 5, 2010, pp. 387-98.
10. Bartus, R.T, *et al.* "The cholinergic hypothesis of geriatric memory dysfunction." *Science*, vol. 217, no. 4558, 1982, pp. 408-14.
11. Mittal, Khyati, and Deepshikha Pande Katare. "Shared links between type 2 diabetes mellitus and Alzheimer's disease: A review." *Diabetes & Metabolic Syndrome:*

Clinical Research & Reviews, vol. 10, no. 2, 2016, pp. S144-S149.
12. Rao, Rammohan, *et al.* "Ayurvedic medicinal plants for Alzheimer's disease: A review." *Alzheimer's research & therapy*, vol. 4, no. 22, 2012.
13. Pullaiah, T. *Encyclopedia of world medicinal plants*. Vol. 1, Regency Publication, 2006. 5 vols.
14. Khare, C.P. *Indian Medicinal Plants: An Illustrated Dictionary*. Springer-Verlag Heidelberg, 2004.
15. Sakthivel, K., *et al*. "Phytoconstituents analysis by GC-MS, cardioprotective and antioxidant activity of *Buchanania axillaris* against doxorubicin-induced cardio toxicity in albino rats." *International Journal of Pharmaceutical Studies and Research*, vol. 1, no. 1, 2010, pp. 34-48.
16. Zarei, Mahsa, *et al*. "Effect of *Hemidesmus indicus* root extract on the blood glucose level in alloxan induced diabetic rats." *Journal of Microbiology and Biotechnology Research*, vol. 3, no. 2, 2013, pp. 64-67.
17. Austin, Anoop. "A Review on Indian sarsaparilla, *Hemidesmus indicus* (L.) R.Br." *Journal of Biological Sciences*, vol. 8, no. 1, 2008, pp.1-12.
18. T, Lakshmi, and Rajendran R. "*Hemidesmus indicus* commonly known as Indian sarasaparilla- an update." *Int J Pharm Bio Sci*, vol. 4, no.4, 2013, pp. 397-404.
19. Thabrew, Ira M., *et al.* "A comparative atudy of the efficacy of *Pavetta indica* and *Osbeckia octandra* in the treatment of liver dysfunction." *Planta Medica*, vol. 53, no. 3, 1987, pp. 239-41.
20. Sheeja, V.N, and S. Subhashini. "Inhibitory action of *Pavetta indica* leaf extracts on the corrosion of mild steel in acid media." *Chemical Science Transactions*, vol. 3, no. 1, 2014, pp.240-254.
21. Nadkarni, A.K. *Indian Materia Medica*. Popular Prakashan. 2 vols.
22. Komersova, Alena, *et al*. "New findings about Ellman's Method to determine cholinesterase activity." *Zeitschrift für Naturforschung. C, Journal of biosciences*, vol. 62, 2007, pp. 150-54.
23. García-Morales, Giovanni, *et al*. "Anti-inflammatory, antioxidant and anti-acetylcholinesterase activities of *Bouvardia ternifolia*: potential implications in Alzheimer's disease." *Archives of Pharmacal Research*, vol. 38, no. 7, 2015, pp. 1369-79.
24. World Health Organization, Regional Office for South-East Asia. Traditional Herbal Remedies for Primary Health Care. 2010. WHO Regional Office for South-East Asia. https://apps.who.int/iris/handle/10665/206024
25. Chetty, Madhava. *Yucca gloriosa Linn: Chittoor medicinal plants*. Himalaya Book Publications, 2005.
26. Benzi, Gianni, and Antonio Moretti. "Is there a rationale for the use of acetylcholinesterase inhibitors in the therapy of Alzheimer's disease?" *European Journal of Pharmacology*, vol. 346, no. 1, 1998, pp. 1-13.
27. Du, Zhi-yun, *et al*. "α-Glucosidase inhibition of natural curcuminoids and curcumin analogs." *European Journal of Medicinal Chemistry*, vol. 41, no. 2, 2006, pp. 213-18.
28. Liu, Yan, *et al*. "Synthesis and pharmacological activities of xanthone derivatives as α-glucosidase inhibitors." *Bioorganic & Medicinal Chemistry*, vol. 14, 2006, pp. 5683-90.
29. Tatsuta, K. "ChemInform abstract: total synthesis and chemical design of useful glycosidase inhibitors." *Pure and Applied Chemistry*, vol. 68, 2005, pp. 283-305.
30. Shaik, J. B., *et al*. "Synthesis, pharmacological assessment, molecular modeling and in silico studies of fused tricyclic coumarin derivatives as a new family of multifunctional anti-Alzheimer agents." *European Journal of Medicinal Chemistry*, vol. 107, 2016, pp. 219-32.
31. Syad AN, Devi KP, "Botanics: a potential source of new therapies for Alzheimer's disease?" Dovepress, 3 April 2014 Volume 2014:4 Pages 11—26.

JOURNAL OF
EMERGING INVESTIGATORS

Article

Effect of the herbal formulation HF1 on the expression of PD-L1 in PC3 cells

Sanah Imani[1], Ankita Umrao[2], Jyothsna Rao[2], Gururaj Rao[2]

[1] The International School of Bangalore NAFL Valley, Whitefield – Sarjapur Road, Bangalore, KA, India, 562125

[2] iCREST-International Stem Cell Services Limited, 9/1, Mission Road, Bangalore

SUMMARY

Cancer is a disease in which abnormal cells divide in an unregulated and uncontrolled fashion, leading to the formation of tumors. One of the mechanisms supporting cancer cell survival is immune evasion. Cancer cells evade the immune system by producing PD-L1, a ligand that is normally produced by non-malignant cells and that interacts with the PD-1 receptor on T cells; this interaction between the PD-L1 ligand and the PD-1 receptor acts like an "off switch" for the production of large amounts of T cells. Though this interaction prevents T cells from attacking normal cells, it also helps cancer cells hide from the immune system. In this *in vitro* study, we aimed to determine whether treatment with a proprietary herbal formulation (HF1; under patent by Sri Raghavendra Biotechnologies Pvt Ltd, Bangalore) affects CD274 gene expression in the prostate cancer cell line, PC3.

We hypothesized that the gene expression of CD274 gene (though we have used protein name, PD-L1 to refer the gene) will be reduced in PC3 cells (a prostate cancer cell line, able to express PD-L1 upon induction) treated with HF1 when compared to PC3 cells that have been induced to express PD-L1. We found that HF1 treatment resulted in a 4-fold decrease in PD-L1 expression when compared to control ($p < 0.001$). Results shows that HF1 and other antioxidants may decrease PD-L1 expression and thus could be useful to develop as a novel cancer therapy.

INTRODUCTION

Tumors are the result of specific genetic mutations that allow cells to grow and spread abnormally (1). There is an immune response to these cancerous cells by both T and B cells. For instance, tumor-infiltrating lymphocytes (TILS) produced in tumor microenvironment, especially CD8+ T cells, have been shown to play a critical role in controlling tumor progression in hepatocellular carcinoma (2).

Programmed death ligand 1 (PD-L1) expression is a mechanism used by tumor cells to evade immunological action. PD-L1 is a 40 kDa, type 1 trans-membrane protein. The proteinplays a significant role in suppressing immune system during inflammatory conditions such as hepatitis (3). PD-L1 works by binding to PD-1, its receptor, which is found on activated T cells and B cells. PD-1 has two potential ligands, PD-L1 and PD-L2. PD-L1 is expressed in many hematopoietic cells and some parenchymal cells, such as pancreatic islet cells and vascular endothelial cells, while PD-L2 expression is linked to macrophages and dendritic cells (DCs) (4).

Once PD-L1 binds to the receptor, the T-cell delivers a signal that inhibits the production of interleukin-2 (IL-2) and cell proliferation. IL-2 is a cytokine that is involved in the process of differentiating T cells into effector T cells and memory T cells, thus helping the body fight infections (5).

In normal tissue, feedback between transcription factors like STAT3 and NF-κB restricts the immune response to protect host tissue and limit inflammation (5, 6). Unlike normal cells, cancer cells exploit this mechanism by upregulating local PD-L1 expression caused bylack of feedback control between transcription factors (7). Furthermore, a phenomenon called T-cell exhaustion occurs, which is characterized by stepwise and progressive loss of T-cell functions (8). The regulation of PD-L1 expression has been connected to various factors. For example, upon interferon gamma (IFNγ) stimulation, PD-L1 is expressed on the surface of T cells, natural killer (NK) cells, macrophages, myeloid DCs, B cells, epithelial cells, and vascular endothelial cells (9).

As a result, novel cancer treatments, such as Nivolumab (Bristol-Myers Squibb), use monoclonal antibodies as an approach to block the interaction between PD-1 and PD-L1 or PD-L2. Another significant area of cancer treatment research is the use of antioxidants like polyphenols to alter cancer growth; however, the effects of antioxidants on immune evasion mechanisms in cancer cells remain poorly understood.

PC3 is a human prostate cancer cell line used in prostate cancer research and drug development. PC3 cells are useful in investigating biochemical changes in advanced

Herbal substance	Anticancer effect
Epigallocatechin-3-gallate (EGCG)	Arrests specific prostate cell lines at the G0-G1 phase (cell cycle). Inhibit metal-loproteinase in vitro. These family of enzymes help in tumor invasion by extra-cellular matrix (ECM) degradation.(10)
Curcumin	Suppressive effect on hepatic fibrogen-esis (fiber formation) and carcinogenesis (tumor formation).(10)

Table 1: Clinical use of herbal medicine exhibiting anticancer activity.

prostate cancer cells and in assessing their response to chemotherapeutic agents (10).

In this investigation, we aimed to determine the effects of HF1, a proprietary herbal formulation, consisting of mainly green tea extract and turmeric, on the expression of PD1 in PC3 cells. Studies have shown that the herbal componentsin HF1 demonstrate anticancer activity (**Table 1**). The polyphenols present in HF1 form an important dietary component and both India and China produce high quality tea, such as Assam tea (11). Green tea and curcumin are significant part of Indian agriculture (12), and therefore makes it a viable option to utilize their anticancer properties and make it accessible to the population as a nutraceutical. One reason for the potential anticancer properties of HF1 is that its components can be oxidized to generate reactive oxygen species (ROS) in cell culture medium and cause cell death (13). It has been demonstrated that administration of EGCG at 0.02%-0.32% in drinking water dose-dependently inhibited small intestinal tumorigenesis in mice (14). In this study, the extent to which HF1 acts as an immune checkpoint inhibitor (15) will be tested *in vitro*. The principle behind immune checkpoint inhibition is to ensure that cancer cells cannot produce PDL1 as they could normally.

RESULTS

IC_{50} value is the dose at which 50% cells would be viable. This dose is important to be known as it provides the toxic dose of a compound. Here, we examined the effect of HF1 on PC3 cells and obtained an IC_{50} value of HF1 using MTT assay to carry out further experiments.

Results shows that 50% cells were viable at 1.27 ± 0.03 mg/mL concentration of HF1 (**Figure 1**). Thus, to prevent cytotoxic effect, HF1 was used at the concentration of half the IC_{50} (1.27 ± 0.03 mg/mL), 0.6 mg/mL.

The levels of PDL1 was studied in various groups by using PCR technique. We examined the effect of HF1 on IFNγ-induced PD-L1 expression in PC3 cells. Treatment with IFNγ (10 ng/mL) increased PD-L1 mRNA levels. However,

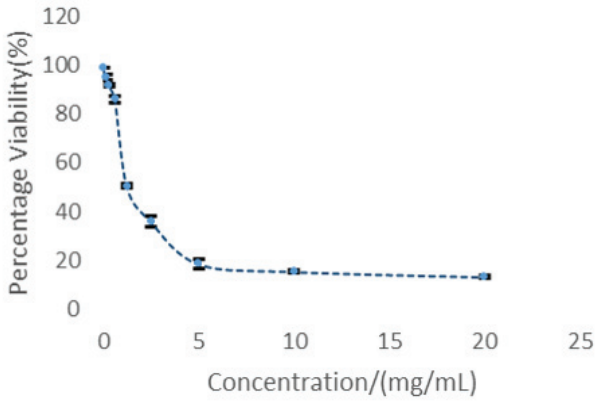

Figure 1: Cytotoxicity effect of HF1 on PC3 cells. A plot of percent viability (%) vs. concentration (mg/mL) of HF1. The obtained IC_{50} was 1.2 mg/mL. Error bars represent standard deviation across three independent sets of experiments.

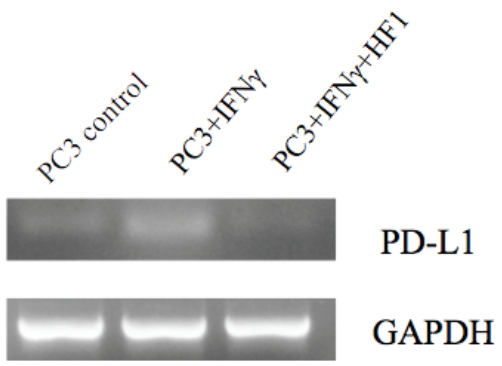

Figure 2: Gel electrophoresis showing expression of PD-L1 and GAPDH (n=3). PC3 control (untreated cells), PC3 cells treated with IFNγ(10 ng/mL) for 24 hours (PC3+IFNγ), PC3 cells treated with IFNγ(10 ng/mL) and HF1 (0.6 mg/mL) (PC3+IFNγ+HF1) for 24h.

treatment with IFNγ and HF1 extract (0.6 mg/mL) lead to a decrease in the levels of PD-L1 mRNA compared to IFNγ treatment alone (**Figures 2 & 3, Table 2**). This shows that antioxidants could be used as a novel therapy in cancer treatment.

mRNA was measured using Quiagen kit. The mRNA expression level of HF1-treated group showed less than one-third of the expression level of the PC3 cells treated with IFNγ (this group represents the state of PD-L1 overexpression found in some cancer cells) (**Figure 3**). The mRNA level in the PC3 cells treated with both IFNγ and HF1 was compared to the PC3 untreated control cells, which served as the baseline of comparison in this experiment.

Expression levels were quantified based on the gel using ImageJ software and were normalized it to GAPDH levels. The PC3+IFNγ group had a fold difference of 6.10 ± 0.40 when normalized against the PC3 control group. In comparison, the PC3+IFNγ+HF1 showed a fold decrease of 1.63 ± 0.18 ($p < 0.001$), which is strikingly close to the baseline expression of PD-L1 considered as in PC3 control group.

To replicate the overexpression found in cancerous cells, the cytokine IFNγ was added to induce ligand expression (18).

DISCUSSION

In this study, we investigated whether HF1, which contains green tea extract and curcumin, modulates PD-L1 levels. We measured PD-L1 mRNA levels in PC3 cells without treatment, with IFNγ alone (10 ng/mL), or with a combination of IFNγ and HF1 (at 0.6 mg/mL, based on the IC_{50} value of 1.2 mg/mL). We chose to study an herbal compound because various studies highlight their antioxidant and anti-cancerous properties (16). For example, the sub-group of polyphenols called gallocatechins (a prominent component of green tea) exertsapoptosis-inducing properties, showing anti-cancer potential. The mechanism of apoptosis induction is quite diverse across different anti-cancerous compounds and is under much study.

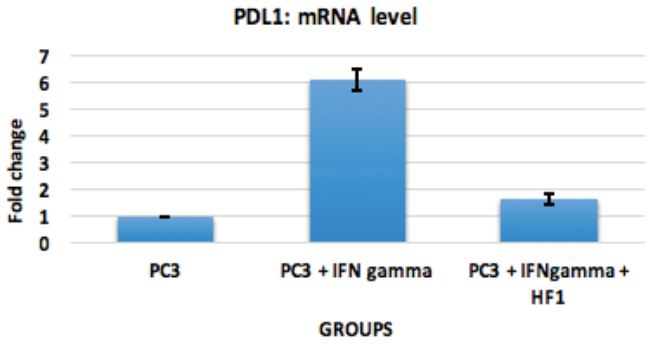

Figure 3: Inhibition of IFNγ-induced PD-L1 by HF1. Inhibition of IFNγ-induced PD-L1 by HF1. PC3 alone was considered as negative control, PC3+IFNγ group was treated with IFNγ (10 ng/mL) and PC3+HF1+IFNγ was treated with both HF1 (0.6 mg/mL) and IFNγ (10 ng/mL). The groups were compared with control.

The PD-1 protein is found on immune cells like T-cells. It functions as an "off switch" that ensures that T cells aren't attacking normal body cells. This protein recognizes PD-L1, a protein found on normal and cancerous cells. This interaction prevents the T-cell attack on the PD-L1-expressing cells. Some cancer cells have large amounts of PD-L1, which helps them hide from immune attack. Hence, lower expression signifies that the tumors may no longer be ableto effectively defend themselves from T cells attack through the PD-1/PD-L1 interaction.

Plant and plant-derived product study is a revolutionary field, as these are simple, safer, eco-friendly, low-cost, fast, and less toxic when compared to conventional treatment methods (17). In addition, active phytochemicals are selective in their functions and act specifically on tumor cells without affecting normal cells (18).

Studies on PD-L1 highlight that the JAK/STAT pathway is associated with regulation (19). Herbal compounds have, in fact, been known to activate and inhibit such cell signaling pathways like MAPK/ERK, making them a prime candidate for PD-L1 regulation, as mentioned previously in reference 17.

The purpose of this investigation was to investigate the effect of an herbal formulation on the expression of the PD-L1 ligand. The hypothesis was that upon addition of a given concentration of the formulation, the expression of PD-L1 would decrease. We also predict (but have not tested) that this will decrease tumor growth and its lifespan as there will be a higher concentration of T cells caused by reduction of PD-L1 on cancer cells.

These results suggest that use of herbal formulations like HF1 can help improve the efficacy of chemotherapy drugs and help by overcoming T cell sweating by down regulating PDL1 expression,and resulting in better efficacy of the treatment. This compound could be tested in a clinical trial wherethe effect of formulation could be studied on cancer patients, with respect to PD-L1 levels. Drug characteristics like absorption, distribution, metabolism, and excretion properties can be deduced andits effects on other cancerous cells that express this ligand need to be studied.

Group	Fold difference of PDL1
PC3	1.00±0.00
PC3+ IFNγ	6.30±0.40
PC3+ IFNγ+HF1	1.63±0.18
The fold difference obtained from three independent experiments conducted for each group of the experiment, with a calculated average and standard error mean (SEM).	

Table 2. Fold difference of PDL1 between groups. The fold difference obtained from three independent experiments conducted for each group of the experiment, with a calculated average and standard error mean (SEM).

METHODS

Cell culture

Cryovials containing the PC3 cells were purchased from NCCS (National Centre for Cell Science), Pune. These vials had a passage number of seven. After rapid thawing, cells were cultured in Dulbecco's Modified Eagle Media (DMEM)/F-12 with 10 % serum (Invitrogen). After centrifugation (1500 rpm, 10 minutes), cells were counted using a hemocytometer, cultured and maintained at 37˚C with 5% CO_2.

At 70-80% confluency, the cells were harvested using 0.25% trypsin-EDTA solution (Invitrogen) and sub-cultured at the density of 0.3 million cells and/or used for MTT assays and PCR.

HF1 Preparation

Hot water decoction was prepared using HF1 powder at the concentration of 0.2 g/mL and was syringe filtered (0.22 µm).

MTT Assay

PC3 cells were plated in a 96-well plate at the density of 3000 cells per well and were incubated at 37˚C with 5% CO_2 levels for 24 hours.

Using serial dilution, a stock of 20 mg/mL of HF1-water extract was diluted to form 8 concentrations ranging from 20 mg/mL to 0.15 mg/mL using DMEM containing 10% serum. Triplicates for each concentration along with appropriate controls (positive control, vehicle control, and media control) were added to respective wells and incubated for 24 hours. Cells were incubated for 4 hours with MTT dye (Sigma)

Gene of Interest	GAPDH
Number of Samples	9
Number of Cycles	30
Denaturation Temperature	94°C
Annealing Temperature	66°C
Extension Temperature	72°C
Description	10 minutes at 95°C; 30 cycles: 94°C for 30 sec, 66°C for 30 sec, 72°C for 45 sec; 72°C for 10 min.

Table 3. PCR information for GAPDH

Gene of Interest	PD-L1
Number of Samples	9
Number of Cycles	30
Denaturation Temperature	94°C
Annealing Temperature	53°C
Extension Temperature	72°C
Description	10 minutes at 95°C; 30 cycles: 94°C for 30 sec, 53°C for 30 sec, 72°C for 45 sec; 72°C for 10 min.

Table 4: PCR information for PD-L1

and DMSO was used to dissolve Formazan crystals. The absorbance of the purple solution was detected at 545 nm using a spectrophotometer (UV10).

Expression and modulation of PD-L1 gene

Cells were counted and cultured in a 6-well plate at a density of 0.3 million cells in 3 mL of media per well. After 24 hours incubation, IFNγ (10 ng/mL) and HF1 (0.6 mg/mL) were added to respective wells, forming three groups: PC3 control (without treatment), PC3+IFNγ, PC3+IFNγ+HF1. Volumes of IFNγ and HF1 used were less than 10%, lower than the toxic dose.

mRNA isolation and cDNA preparation

After another 24 hours of incubation, the cells were trypsinized, centrifuged, and then the mRNA was isolated (Qiagen RNA isolation kit). mRNA was quantified and purity was determined using spectrophotometer at two wavelengths: 260 nm and 280 nm.

cDNA preparation

DEPC-treated tubes were used to prepare cDNA using Genie RT PCR kit. The standard protocol included addition of Oligo-dT, RNasin, DTT, dNTPs, MULV reverse transcriptase, and assay buffer to the mRNA samples.

The samples were incubated at 37°C for an hour, centrifuged at 12000 rpm (usually for a short spin of 15 seconds), and stored at -80°C for further use.

Semi-quantitative PCR

After calculating the appropriate cDNA volumes (to ensure a concentration of 200 ng cDNA/50 µL PCR reaction), PCR reactions were set up with 12.5µL of the Jumpstart mix (Sigma), 1 nM of GAPDH forward and reverse primer (Eurofins) and the remaining volume of molecular grade water (**Tables 3 & 4**).

Gel Electrophoresis

5 µL of each PCR product was mixed with 2 µL of 6X gel loading dye (Sigma) before adding to the wells in a 3% agarose gel. 100 bp DNA ladder was also loaded. The gel was run for one and a half hours at 50 V.

Each gel image was exported and analyzed using ImageJ. LUT was inverted so that the bands were black and the background was subtracted. The bands of interest were isolated using the rectangle tool. The band intensity peaks were plotted and the peaks were separated using the line tool. The area under each peak was measured for the housekeeping gene GAPDH and PD-L1 gene. PD-L1 mRNA level was normalized with the respective GAPDH level in each group.

We measured the fold change for normalized PD-L1 gene expression across the experimental groups: control, PC3+IFNγ, and PC3+IFNγ+HF1.

This fold difference can also be seen through the images produced through the ImageJ software. As mentioned earlier, the measure of area under the curve for each group is correlated with expression.

Data analysis

To check experimental reliability, three independent sets of the same experiment were performed.

The PD-L1 mRNA levels were normalized with the GAPDH levels by taking the PD-L1 to GAPDH ratio for each corresponding sample. These normalized values were then compared to the PC3 control values by taking the ratio of the levels of each group with PC3 control group values.

$$arithmetic\ mean = \frac{\sum_{n=1}^{k} x_n}{k}$$

An average value was calculated across the three trials for each group. The standard arithmetic average formula is used here (20).

The error bars represent the standard error of the mean (SEM). It indicates the spread that the mean of a sample of the values would have if you kept taking samples.

SEM is calculated by taking the standard deviation and dividing it by the square root of the sample size (21).

$$standard\ deviation\ \sigma = \sqrt{\frac{\sum_{i=1}^{k}(x_i - x_{avg})^2}{n-1}}$$

$$standard\ error = \frac{\sigma}{\sqrt{n}}$$

Using the GraphPad software, OneWay ANOVA was used to compare the means of the three groups. The output was a *p*-value of 0.001 was obtained. This shows that the difference between the means are statistically significant as conventionally a *p*-value < 0.05 shows high statistical significance.

Received: June 25, 2019
Accepted: November 6, 2019
Published: November 15, 2019

REFERENCES

1. Moasser, M M. "The oncogene HER2: its signaling and transforming functions and its role in human cancer

pathogenesis." *Oncogene*, vol. 26, no. 45, 2007, 6469-87. doi:10.1038/sj.onc.1210477
2. Yeong, J, *et al*. "Original Article: Interaction between Tumour-Infiltrating B Cells and T Cells Controls the Progression of Hepatocellular Carcinoma." *Gut*, vol. 66, no. 2, 2015, doi: 10.1136/gutjnl-2015-310814.
3. Wang, Yiting *et al*. "Regulation of PD-L1: Emerging Routes for Targeting Tumor Immune Evasion." *Frontiers in Pharmacology*, vol. 9, no. 536, 2018, doi:10.3389/fphar.2018.00536
4. Zitvogel, Laurence, and Guido Kroemer. "Targeting PD-1/PD-L1 interactions for cancer immunotherapy." *Oncoimmunology*, vol. 1, no. 8, 2012. doi:10.4161/onci.21335
5. Song, Tammy Linlin *et al*. "Oncogenic activation of the STAT3 pathway drives PD-L1 expression in natural killer/T-cell lymphoma." *Blood*, vol. 132, no. 11, 2018. doi:10.1182/blood-2018-01-829424
6. Asgarova, A *et al*. "PD-L1 expression is regulated by both DNA methylation and NF-kB during EMT signaling in non-small cell lung carcinoma." *Oncoimmunology*, vol.7, no. 5, 2018. doi:10.1080/2162402X.2017.1423170
7. Vlahopoulos, Spiros A. "Aberrant control of NF-κB in cancer permits transcriptional and phenotypic plasticity, to curtail dependence on host tissue: molecular mode." *Cancer Biology & Medicine*, vol. 14, no. 3, 2017. doi:10.20892/j.issn.2095-3941.2017.0029
8. Yi, John S, *et al*. "T-Cell Exhaustion: Characteristics, Causes and Conversion." *Immunology, Blackwell Science Inc*, vol. 129, no. 4, 2010, doi: 10.1111/j.1365-2567.2010.03255.x.
9. 9. Riella, L V, *et al*. "Role of the PD-1 Pathway in the Immune Response." *American Journal of Transplantation*, vol. 12, no. 10, 2012. doi: 10.1111/j.1600-6143.2012.04224.x.
10. Tai, Sheng *et al*. "PC3 is a cell line characteristic of prostatic small cell carcinoma." *The Prostate*, vol. 71, no. 15, 2011. doi:10.1002/pros.21383.
11. Baruah, P. "Types of Indian Tea, Production and Marketing of Traditional and Handmade Teas of Assam, India." *Journal of Tea Science Research*, vol. 7, no. 10, 2017.doi: 10.5376/jtsr.2017.07.0010
12. Shi, Qin-Yin, and Vicki Schlegel. "Green Tea as an Agricultural Based Health Promoting Food: The Past Five to Ten Years." *MDPI, Multidisciplinary Digital Publishing Institute*, vol. 2, no. 4, 2012. doi: https://doi.org/10.3390/agriculture2040393.
13. Hou, Zhe, *et al*. "Mechanism of Action of (−)-Epigallocatechin-3-Gallate: Auto-Oxidation–Dependent Inactivation of Epidermal Growth Factor Receptor and Direct Effects on Growth Inhibition in Human Esophageal Cancer KYSE 150 Cells." *Cancer Research*, vol. 65, no. 17, 2005.doi: 10.1158/0008-5472.CAN-05-0480.
14. Ju, Jihyeung, *et al*. "Inhibition of Intestinal Tumorigenesis in Apcmin/ Mice by (−)-Epigallocatechin-3-Gallate, the Major Catechin in Green Tea." *Cancer Research*, vol. 65, no. 22, 2005. doi:10.1158/0008-5472.CAN-05-1949.
15. Darvin, Pramod, *et al*. "Immune Checkpoint Inhibitors: Recent Progress and Potential Biomarkers." *Nature News*, vol. 50, no. 2, 2018.doi: 10.1038/s12276-018-0191-1.
16. Yin S-Y, Wei W-C, Jian F-Y, Yang N-S. "Therapeutic Applications of Herbal Medicines for Cancer Patients". *Evid Based Complement Alternat Medicine*, vol. 1, 2013. doi:10.1155/2013/302426.
17. Yang, Chung S et al. "Effects of Tea Catechins on Cancer Signaling Pathways." *The Enzymes*. vol. 36, 2014. doi:10.1016/B978-0-12-802215-3.00010-0
18. "Plant-Derived Anticancer Agents: A Green Anticancer Approach." *Asian Pacific Journal of Tropical Biomedicine*, vol. 7, no. 12, 2017. doi: 10.1016/j.apjtb.2017.10.016.
19. Mimura, Kousaku *et al*. "PD-L1 expression is mainly regulated by interferon gamma associated with JAK-STAT pathway in gastric cancer." *Cancer Science*. vol. 109, no. 1, 2018. doi:10.1111/cas.13424
20. Manikandan, S. "Measures of Central Tendency: The Mean." *Journal of Pharmacology & Pharmacotherapeutics*, vol. 2, no. 2, 2011. doi: 10.4103/0976-500X.81920.
21. Barde, Mohini P, and Prajakt J Barde. "What to Use to Express the Variability of Data: Standard Deviation or Standard Error of Mean?" *Perspectives in Clinical Research*, vol. 3, no. 13, 2012. doi: 10.4103/2229-3485.100662.

JOURNAL OF
EMERGING INVESTIGATORS

Article

The effects of vibrotactile feedback on task performance in a 3D-printed myoelectric prosthetic arm

Sidney Nguyen, Henrik Malmberg
The Westminster School, Atlanta, GA

SUMMARY

The lack of tactile feedback in today's hand prosthetics complicates the user experience by forcing a user to visually confirm that the prosthetic is grasping an object. This study strives to remedy both the financial and mechanical deficiencies in current prosthetics through building a simple, noninvasive, vibratory sensory feedback system into an inexpensive constructed 3D-printed prosthetic arm. This 3D-printed prosthetic arm was designed in SolidWorks and printed to the specifications of a participant with a left forearm amputation. The myoelectrical components include a muscle sensor that sends electrical signals to an Arduino microcontroller, which translates the data into code orders to trigger a servo motor to open or close the hand. Vibrotactile feedback was implemented by using a touch sensor on the tip of the index finger of the prosthetic that activates a vibrating motor attached to the residual arm. To test the efficacy of the sensory feedback, the participant was asked to perform a series of tasks both with and without the vibrotactile feedback, both blindfolded and non-blindfolded. The presence of vibrotactile feedback was essential for completing blindfolded tasks, but it did not assist in improving non-blindfolded task performance. The total cost of materials to build this prosthetic arm was $158.46. This study supports the hypothesis that the simple sensory vibrotactile feedback system in the design of this 3D-printed myoelectric prosthetic arm has the potential to enhance sensory feedback performance of amputees by decreasing visual dependency, at a fraction of the cost of a custom-designed myoelectric prosthetic.

INTRODUCTION

According to the nonprofit Amputee Coalition, of the two million amputees living in the United States, 350,000 suffer from upper limb loss (1). While a single prosthetic that achieves both a natural appearance and extreme functionality would be ideal, most artificial limbs that exist today sacrifice one for the other in varying degrees.

The major prosthetic categories for upper limbs include cosmetic, body-powered, and myoelectric prosthetics. Cosmetic prosthetics have little to no functional use and are made primarily of silicone to resemble the user's original limb appearance (2). The lack of mechanical functionality yields a relatively lightweight prosthetic, as the mechanical components are not required. In terms of cost, they are the most affordable prosthetics.

Body-powered prosthetics rely on a system of cables or harnesses to control the prosthetic limb by moving other parts of the body, such as the shoulder girdle, elbow, and chest. Moving the body parts in a certain way will pull on the cable and cause the prosthetic hand to open or close (3). While they are highly durable, the body-powered prosthetic requires unnatural movements of the connected body parts, which can make movements awkward for the user (4). Over time, the prosthetic straps and cables can become uncomfortable and difficult to operate and will need ongoing adjustments and repairs (5).

Externally powered artificial limbs such as myoelectric prosthetics are an attempt to solve the physical exertion issue by using a battery and an electronic system to control movement. Myoelectric prosthetics, unlike body-powered prosthetics, do not require any straps or harnesses to function, thus providing a more natural appearance. They are custom made to fit the remaining limb. The prosthetic's movement is initiated by muscle contractions on the residual limb, which alter resistance in muscle detector sensors. This information is relayed to a microprocessor, which deciphers the readings and instructs a servo motor to turn and adjust the position of the fingers to open and close the hand (6). Currently, the main disadvantages of myoelectric prosthetics are their weight and cost (7). Myoelectric prosthetics tend to be heavier because of the required hardware for operation. While they are more expensive than other kinds of prosthetics, they offer the best quality regarding both cosmetics and functionality.

Rudimentary myoelectric prosthetics close the entire prosthetic hand when a single muscle contraction is detected, which greatly increases its initial ease of use. Advanced myoelectric prosthetics use multiple sensors and motors activated by different muscle contractions on the residual limb to allow for control of individual fingers. Extensive training and knowledge are necessary for the user to effectively use this type of prosthetic (8).

The functionality of a prosthetic plays a vital role in the selection process, as does the cost. On average, a cosmetic prosthetic costs between 3,000 to 5,000 USD; a body-powered prosthetic costs around 10,000 USD; and a commercial myoelectric prosthetic can range in cost from 20,000 to 100,000 USD (9). Commercial 3D-printed

myoelectric prosthetics, such as the Dexterous Hand by Shadow Robot Company and the Hero Arm by Open Bionics, are considered the more affordable myoelectric alternatives, with prices as low as 2,500 and 6,500 USD, respectively (10, 11). The reduced cost of these 3D-printed prosthetics has proven especially beneficial for children, as with continued growth and use, children frequently require prosthetics to be repaired, replaced, and re-fitted. We decided to use 3D printing to manufacture the device in this study primarily due to its affordability.

Upper limb prosthetics remain limited in complex motor and sensory feedback despite the advancements in prosthetic technology and cost associated with prosthetics. Sensory feedback is critical in restoring functionality to amputees, as it would relieve the cognitive burden of relying solely on visual input to monitor motor commands. Already in use is a technique called sensory substitution in which one type of sensation is substituted for another. For example, vibration applied to the skin of the remaining limb, or to another part of the body, is used to convey touch from sensors on the prosthetic. Vibrotactile stimulation through sensory substitution was the sensory feedback system of choice incorporated in this research as it is inexpensive, noninvasive, and could be easily implemented into myoelectric prosthetic technology (12).

Other methods of feedback include various types of implanted neural interfaces—electrodes implanted in the proximity of the residual nerves of the amputated arm—which are activated by sensors on the prosthetic. This direct neural stimulation approach shows promise for enabling patients to detect object characteristics including size, shape, and stiffness to control fine motor movements without visual cues (13). Current approaches in testing seek to avoid implanted nerve electrodes by using a technique called sensory regenerative peripheral nerve interface (sRPNI), in which a "bioartificial interface" transfers sensory signals directly from a prosthetic sensor to the remaining nerve (14). However, despite their promise, we were not able to explore these new technologies in this study due to limited funds.

The purpose of this study is to determine the efficacy of a vibratory tactile feedback system placed on the index finger of an inexpensive constructed 3D-printed myoelectric prosthetic arm in performing various tasks. We were able to construct the prosthetic with a total materials cost of $158.46. We evaluated the efficacy of the vibrotactile feedback by having a participant with a left forearm amputation wear the constructed 3D-printed myoelectric prosthetic arm while performing functional tests, non-blindfolded and blindfolded, with and without vibrotactile feedback. The presence of vibrotactile feedback proved essential for completing blindfolded tasks. However, vibrotactile stimulation did not improve task performance when the participant had the aid of vision. At a fraction of the cost of a custom-designed myoelectric arm, the design of this 3D-printed myoelectric prosthetic arm has the potential to enhance sensory feedback performance for the amputee using a simple sensory vibrotactile feedback system.

RESULTS

Construction of the 3D-Printed Myoelectric Prosthetic Arm

This 3D-printed myoelectric prosthetic arm was designed to the specifications of a participant with a left forearm amputation. The prosthetic was then designed in a 3D modeling software, Solidworks. The phalanges of the fingers went through five prototypes before the final design. Once the CAD designs were completed, the models were 3D printed using ABS plastic**.** The prosthetic utilized an Arduino microcontroller in tandem with a servo and a MyoWare muscle sensor to control the grasping motion**.** An additional feedback system was integrated into the index finger which gave the user feedback by way of a vibrating motor **(Figure 1a-d)**.

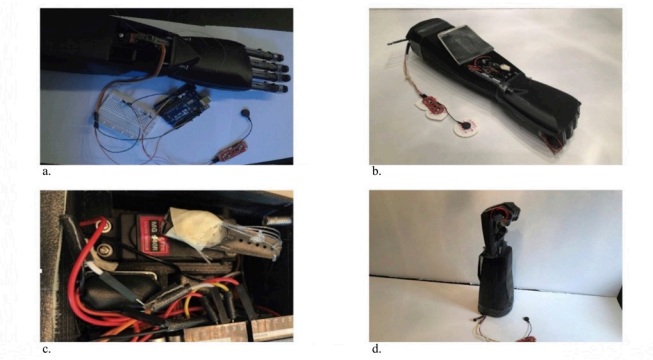

Figure 1: Images of completed 3D printed myoelectric prosthetic. (a) electronic components before assemble, (b) electronic components housed in forearm, (c) close up of electronics housing, (d) complete 3D printed prosthetic arm.

Task Performance Testing

Testing was conducted by asking the participant to complete a series of tasks while blindfolded and non-blindfolded **(Figure 2a-f)**. To evaluate the efficacy of the vibrotactile feedback system, each task was performed 5 times under consistent conditions with and without the vibrotactile feedback. The average of the 5 values was taken as the final performance metric for each task. Failure to complete a task is defined as taking longer than 60 seconds. The paired sample t-test in Microsoft Excel was used to compare the statistical difference between the time taken to perform the tasks with the presence and absence of vibrotactile feedback while blindfolded and non-blindfolded.

Blindfolded Tasks

Vibrotactile feedback efficiency was evaluated by observing the participant's completion of three simple tasks while blindfolded. The absence of the vibrotactile feedback resulted in significant failure to complete all three tasks ($p<0.001$) while blindfolded. The participant failed to detect the presence of the block on her palm, locate the block on the

tray, or determine if her prosthetic was being touched. With vibrotactile feedback activated, the participant successfully completed all three tasks **(Table 1a, 1b)**.

Figure 2: 3D printed myoelectric prosthetic arm conducting various non-blindfolded tasks. (a) Pick up a light object/plastic cube, (b) pick up a heavy object/ sampler, (c) hold a cup, (d) pick up bottle and transfer to tray, (e) pick up travy, (f) squeeze a toothpaste onto toothbrush.

Blindfolded Tasks		**Trials (seconds)**					
Trial Number		1	2	3	4	5	Average
With VF	Detect if index finger with tactile sensor was touched	2	1	1	2	1	1.4
	Detect block on palm with fingers closed	15	16	13	10	8	12.4
	Locate block on tray	27	25	30	24	34	25.8
Without VF	Detect if index finger with tactile sensor was touched	F	F	F	F	F	F
	Detect block on palm with fingers closed	F	F	F	F	F	F
	Locate block on tray	F	F	F	F	F	F

Table 1a: Blindfolded tasks performed with and without vibrotactile feedback over 5 trials.

Blindfolded Tasks	**Without VF Mean time (s)**	**With VF Mean Time (s)**	**p-value**
Detect if index finger with tactile sensor was touched	F	1.4	<0.001
Detect block on palm with fingers closed	F	12.4	<0.001
Locate block on tray	F	25.8	<0.001

Table 1b: Comparison of blinded tasks performed with and without vibrotactile feedback. Failure= F(Is defined as 60 seconds or more)

Non-blindfolded Tasks

There was no statistical significance in efficiency of task performance observed with vibrotactile feedback or without vibrotactile feedback in the absence of a blindfold (p> 0.05). In either case, the participant was able to successfully pick up a light plastic cube (20 g) and a heavy stapler (500 g), to hold a cup, pick up a bottle and transfer it onto a tray, to hold a tray, and to squeeze toothpaste onto a toothbrush. Fine motor task completion, such as picking up a coin and cutting food, was an overall failure regardless of whether the vibrotactile feedback was present **(Table 2a, 2b).**

Cost of Constructing the 3D-Printed Myoelectric Prosthetic Arm

The total cost of all the materials required to construct this 3D-printed myoelectric prosthetic arm, all of which could be purchased on Amazon, was $158.46 **(Table 3)**.

Unblindfolded Tasks		**Trials (seconds)**					
Trial Number		1	2	3	4	5	Average
With VF	Pick up a coin	F	F	F	F	F	F
	Cutting food	F	F	F	F	F	F
	Pick up a light object (plastic cube = 20 g)	40	38	36	41	35	38.0
	Pick up a heavy object (stapler = 500 g)	12	15	14	12	13	13.2
	Hold a cup	10	11	12	8	14	11.0
	Pick up a bottle and transfer it onto a tray	52	47	43	45	48	47.0
	Hold a tray	15	16	19	20	13	16.6
	Squeeze toothpaste onto toothbrush	55	60	50	46	48	51.8
Without VF	Pick up a coin	F	F	F	F	F	F
	Cutting food	F	F	F	F	F	F
	Pick up a light object (plastic cube = 20 g)	42	45	38	39	37	40.2
	Pick up a heavy object (stapler = 500 g)	11	13	15	19	12	14.0
	Hold a cup	8	9	12	11	13	10.6
	Pick up a bottle and transfer it onto a tray	53	50	47	45	48	48.6
	Hold a tray	13	14	17	14	16	14.8
	Squeeze toothpaste onto toothbrush	51	53	49	48	43	48.8

Table 2a: Non-blindfolded tasks performed with and without vibrotactile feedback over 5 trials.

Unblindfolded Tasks	**Without VF Mean Time (s)**	**With VF Mean Time (s)**	**p-value**
Pick up a coin	Failure	Failure	N/A
Cutting food	Failure	Failure	N/A
Pick up a light object (plastic cube = 20 g) **(Figure 1a)**	40.2	38.0	0.09
Pick up a heavy object (stapler = 500 g) **(Figure 1b)**	14.0	13.2	0.2
Hold a cup **(Figure 1c)**	10.6	11.0	0.1
Pick up a bottle and transfer it onto a tray **(Figure 1d)**	48.6	47.0	0.05
Hold a tray **(Figure 1e)**	14.8	16.6	0.1
Squeeze toothpaste onto toothbrush **(Figure 1f)**	48.8	51.8	0.06

Table 2b: Comparison of non-blindfolded tasks performed with and without vibrotactile feedback.

Materials	**Cost**
HATCHBOX 1.75mm White PLA 3D Printer Filament - 1kg Spool - Dimensional Accuracy +/- 0.05mm	$19.99
MyoWare Muscle Sensor	$37.99
Elegoo EL-KIT-004 UNO Project Basic Starter Kit with Tutorial and UNO R3 for Arduino	$17.65
5pcs DC3V/0.1A 1.5V/0.05A 10x2.7mm Coin Mobile Phone Vibration Motor	$5.28
Energizer Max Alkaline 9 Volt, 4-Count	$10.38
RioRand MG946R High Torque Servo for Motor Helicopter Boat Model.	$9.90
3M Red Dot Foam Monitoring Electrode, 4.4 cm Diam., 50/Bag, 3M9640	$12.84
Orthodontic bands	$5.50
Energizer Max Alkaline AAA, 4-Count	$3.74
10 Pieces Black Latching self locking 1A push button on off micro mini 1208YD B5	$10.00
10-32 x 1" Button Head Socket Cap Screws, Allen Socket Drive, Stainless Steel 18-8, Full Thread, Bright Finish, Machine Thread, Quantity 50 By Fastenere	$12.20
Striveday™ 30 AWG Flexible Silicone Wire Electric wire 30 gauge Coper Hook Up Wire 300V Cables electronic stranded wire cable electrics DIY BOX-1	$12.99
Total cost	**$158.46**

Table 3: Breakup cost of materials used for constructing the 3D-printed myoelectric prosthetic arm with vibrotactile feedback.

DISCUSSION

New technological advancements in the field of myoelectric prosthetics have led to the development of hands with multiple degrees of freedom of movements. Unfortunately, current upper limb prosthetics are still limited in terms of complex motor control and sensory feedback. The lack of sensation is the key limitation to reestablishing the full functionality of the natural limb. Providing some sense of touch to the artificial hand would lessen the cognitive burden of relying solely on vision to initiate and monitor movements. Sensory substitution, the vibrotactile feedback modality used in this myoelectric prosthetic arm, is simple, inexpensive and noninvasive but has major limitations. During ordinary wear over time, sweat can impede the connection between the

electrode and the skin, so that the user feels less or even no feedback at all. This limitation was exhibited during testing, which necessitated changes of electrode pads to enhance better adherence to the skin. Additionally, in this iteration, the vibrotactile feedback was present only on the index finger of the prosthetic. This could be improved by having touch sensors in multiple areas, such as the palm and fingers.

The participant failed to complete two fine motor tasks, including cutting food and picking up a coin, with or without the presence of vibrotactile feedback. The failure to cut food can be attributed to the lack of wrist articulation. Because of the absence of a wrist joint in the design of this prosthetic, the participant is relegated to performing tasks in which the object can be grasped or held perpendicular to the forearm. Though this orientation can be rotated to hold objects vertically or horizontally, which encompasses many daily activities, the inability to properly hold a knife reveals a more overarching limitation. The participant was able to complete the remaining tasks regardless of the locked wrist.

The participant's inability to pick up a coin is caused by the deliberate design of the fingers. Because of the design of the control system, in which the muscle sensor activation results in the simultaneous closing of the hand, the hand would excel at picking up larger everyday objects rather than manipulating much smaller objects with individual fingers. Knowing this beforehand, the fingers were designed with large rubber tips to further strengthen the prosthetic's ability to pick up larger objects.

The prosthetic excelled particularly at picking up cylindrical objects such as a bottle or a cup. This ability can be attributed to the curved surface of the palm, which was designed to emulate the curved nature of a clenched hand. The prosthetic continues to retain the ability to grasp angular objects due to its relatively gradual curve.

Throughout the testing, once the participant was able to grasp an object, the participant would not involuntarily lose control of the object. The participant used a toggle system, where a muscle contraction detected by the muscle sensor on the residual limb would cause the hand to close and another would cause a release. Prior to the addition of the toggle control, in personal testing, the participant found difficulty in retaining an object in the prosthetic's grip once picked up, as it required constant muscle contraction to remain in the closed state.

The participant did not report unintentional activations post calibration. Previous versions that excluded an average of the sensor values resulted in sporadic control and unintentional activations. These unintentional activations were caused by the sensor over exaggerating abrupt minute changes in sensor values while the participant was resting her muscle.

Some more complex prosthetics use multiple sensors positioned at muscles along the residual limb to detect multiple different signals and allow the user to individually actuate each finger, resulting in a more accurate emulation of a human hand. This prosthetic used a single muscle sensor to detect a single muscle contraction to simultaneously close all the fingers of the hand. The simplicity of a single muscle stimulation may prove beneficial in reducing the time required to master the use of a prosthetic in comparison with more advanced options. Though a single sensor reduces the learning curve, the simultaneous closing of all five fingers is a notable limitation since each finger cannot be individually controlled. Future iterations could use five separate muscle sensors and five servos to allow for independent movement for each finger. This will, however, not only increase the weight but the overall cost in producing the prosthetic.

This study utilized only one participant who performed each task five times to determine the efficacy of the vibrotactile feedback of the 3D-printed myoelectric prosthetic arm. While relegating the various performance tasks to only a single participant ensured the data between activated and deactivated vibrotactile feedback would be comparable, the small sample size decreased statistical power and inflated false discovery rate. Future iterations could utilize multiple participants as this would provide data on how the prosthetic performs on different people and can expose shortcomings that are not immediately evident on the participant in this study.

Testing other available prosthetics could provide data on the effectiveness of this prosthetic relative to its prospective competitors. This prototype aims to replicate the function of more costly commercial myoelectric prosthetics. A participant performing identical tasks using this prosthetic as well as other different myoelectric prosthetics could compare the shortcomings and advantages of each option. Comparable testing using other commercial prosthetics was not done in this study because of cost restrictions.

This study found that the presence of vibrotactile feedback proved to aid the participant only in situations with complete absence of vision. Future testing could assess the effectiveness of the vibrotactile feedback in different environments with varying degrees of brightness. Replicating the same tests in varying lower visibility settings would demonstrate the effects of different levels of darkness has on the user and vibrotactile feedback's ability to change the user's performance. Another way to test the user's performance in a reduced visibility environment would be controlling the prosthetic with decreased peripheral vision. The user could attempt to complete the tasks while looking straight ahead and performing each task on the edge of their peripheral vision or at the corner of their eyes.

All the materials required to construct this 3D-printed myoelectric prosthetic arm were purchased on Amazon for $158.46 **(Table 5)**. Commercial myoelectric prosthetics can cost around $20,000 to $100,000. The more affordable commercial 3D-printed myoelectric prosthetic arms can range between $2,500 to $6,500. While many patients cannot afford the most cutting-edge technology, demand for prosthetic-and promising techniques from the 3D-printing industry may make them more affordable.

The absence of the vibrotactile feedback resulted in

significant failure to complete all three tasks while blindfolded; the participant was able to successfully complete the three blindfolded tasks with vibrotactile feedback activated (p<0.001). There was no significant statistical increase in efficiency of task performance observed with or without vibrotactile feedback in the absence of a blindfold (p>0.05). This study provides evidence that vibrotactile feedback enhances the user's performance in situations in the absence of vision. This inexpensive 3D-printed myoelectric prosthetic arm has the potential to enhance sensory feedback performance of amputees and provide a substitution to the amputated limb, at a fraction of the cost of a custom-designed commercial myoelectric prosthetic.

MATERIALS AND METHODS

Construction of a 3D-Printed Myoelectric Prosthetic Arm with Vibrotactile Feedback for a Participant with Left Forearm Amputation

Measurements of the Participant's Limb

Participant: A left forearm amputee participated in the study. An Institutional Review Board (IRB) at The Westminster School approved the experimental protocol. Informed consent was obtained from the subject.

The process of designing this 3D-printed myoelectric prosthetic arm began with measuring the participant's left amputated forearm residual limb. The intact right arm was also measured for comparison.

Computer Assisted Drafting (CAD)

The original 3D-printed prosthetic arm designed for the participant with a left forearm amputation was created using a computer aided drafting (CAD) software called SolidWorks by drawing 2D sketches and extruding those sketches into 3D objects.

Fingers: Fourteen individual phalanges were created. The thumb had 2 phalanges, while each of the remaining four fingers had proximal, middle, and distal phalanges. All followed the same design concept in which an original 0.6 by 0.6 square was extruded to the desired length of each phalange. To create the curved appearance, symmetric fillets on the remaining edges of the prism were added. The phalanges of each finger were linked by a series of joints and pins. A small hole ran through each phalange that corresponded to the next so that the fishing line that acted as a "tendon" could be threaded through the phalanges to form the fingers **(Figure 3a, 3b).**

Optimal functionality of the prosthetic fingers was achieved through the trial and error of five phalange prototypes. In the first iteration, joint fulcrum placement was initially below an overhanging cosmetic cover, which resulted in the fishing line "tendon" placement above the joint. Subsequently, flexing the fingers would rely solely on orthodontic bands. Using the force provided by orthodontic bands to grasp ultimately wasted the servo's power by relegating it to opening the hand and overcoming the minimal force provided by orthodontic bands. The first iteration's **(Figure 4; V1)** reliance on orthodontic bands to close the hand and its omission of mounts for the bands made the fingers non-functional.

Figure 3: 3D models of various 3D prosthetic components: (a) distal phalange, (b) assembled proximal and distal phalanges, (c) palm, (d) forearm, (e) palmer aspect of assembly, (f) dorsal aspect of assembly.

The second iteration **(Figure 4; V2)** repositioned the joint fulcrum, which allowed the orthodontic bands to open the hand and used the servo's power to flex the fingers to close the hand. However, this prototype lacked orthodontic band mounts.

The third prototype **(Figure 4; V3)** introduced the first iteration with orthodontic band mounts, which involved creating channels on the top of each phalange. This iteration was the first fully functioning prototype that used the servo's power to flex the fingers and orthodontic bands to extend the fingers to open the hand. The channels, however, were large relative to future iterations. The large channels allowed the bands to pop out easily; therefore, "caps" were introduced. The caps proved problematic, as they were bulky, and friction fitted with minimal tolerance between the cap and the phalange; hence, it required a vice for installation. The "caps" were difficult to work with, because they tended to snap during removal and installation. When they did not snap, the necessity for a vice and pliers was tedious and complicated the process. These factors led to the creation of Version Four.

The fourth iteration **(Figure 4; V4)** reduced the width at the top of the channel and widened the gap towards the bottom. This design trapped and secured the orthodontic bands once they were installed. The reduced gap size increased the difficulty of mounting the orthodontic bands into the channel but held them without the need for "caps."

The final prototype, **(Figure 3a, 5)** utilized the same tapered channel design of the previous iteration, with a larger gap at the front of the channel to allow for easier insertion of orthodontic bands. The increased tolerance between the joint and pin eliminates the need for sanding.

Palm: The palm was dimensioned to the size of the participant's existing right palm. The design for the palm was based around spacing the fingers 1.6 cm. apart while keeping the overall width 9 cm. and the length 10 cm. While each finger was identical in length, the palm's mounting joints were staggered, leaving each finger at a different level in order to

emulate a real hand. Keeping the finger lengths the same, shortens the design of time of having to design 5 fingers of various lengths. At the bottom of the palm, a slight curve was implemented to more closely resemble the closed hand and allow for more effective grasping. The five fishing lines for the five fingers were threaded through the five tunnels inside the palm, threaded through the forearm, and grouped together to attach to the servo arm. Four tap size 10-32 holes were made on the back of the palm to bolt it to the forearm **(Figure 3c)**.

Forearm: The forearm consisted of two major compartments: a sleeve to accommodate for the participant's amputated forearm/stump and the electronics-housing compartment. Additional paddings were inserted between the prosthetic arm sleeve and the participant's arm to ensure the device stayed on the residual limb and provide comfort for the user. The electronics-housing compartment was further subdivided into two separate spaces to secure the 5-volt servo and the 9-volt battery. The remaining space housed the Arduino, AAA battery, and electrical wiring (**Figure 3d, 3e, 3f**).

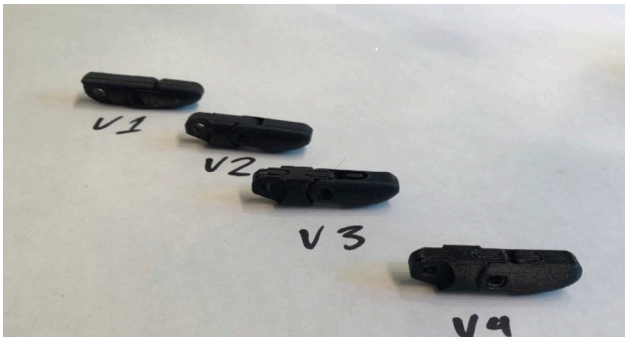

Figure 4: 3D-printed versions (V) of the distal and middle phalanges V1 to V4.

3D-Printing

Acrylonitrile butadiene styrene (ABS) filament was used for the printing of this prosthetic arm. It requires a heated bed to prevent the outer layers from curling in or wrapping, which guarantees an even distribution of heat to both inner and outer layers (15). By nature, ABS plastic also shrinks following a print or injection mold. Therefore, the prosthetic's size was over-exaggerated in the g-code to compensate for the 8.5% shrinkage. The 3D-printed components of the prosthetic hand—the palm and the proximal, middle, and distal phalanges—are shown in **(Figure 5)**. The 3D-printing data of this prosthetic arm is represented in **(Table 1).**

MyoWare Muscle Sensor

The MyoWare Muscle Sensor was applied to the skin directly on top of the muscle of the residual limb. It uses electromyography (EMG) to measure the electrical activity of the muscle contraction and converted the data into varying voltages that could be understood by electronic devices such as Arduino microcontrollers. The connections and the electrical circuitry between the MyoWare Muscle Sensor, Arduino, servo, and 9-Volt battery are shown in **(Figure 6,**

Figure 5: Unassembled 3D- printed components palm proximal, middle, and distal phalanges.

Part Name	Print Time (Minutes)	Infill Percentage	Layer Height
Distal Phalange V1	69	50	3
Distal Phalange V2	58	50	3
Distal Phalange V3	60	50	3
Distal Phalange V4	61	50	3
Distal Phalange V5	63	50	3
Medial Phalange V5	57	50	3
Proximal Phalange V5	70	50	3
Palm	873	20	5
Forearm	4320	20	5

Table 4: 3D- Printing data of the prosthetic arm.

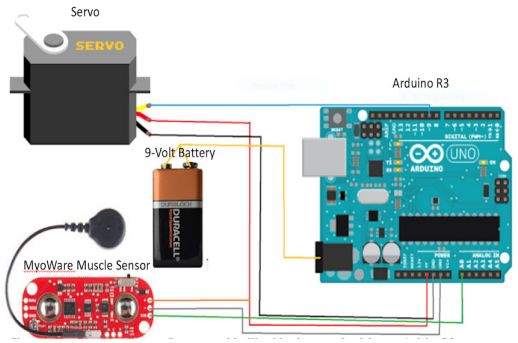

Figure 6: Circuitry wiring diagram, Components: MyoWare Muscle sensor, 9-volt battery, Arduino R3, servo motor.

Color	Length (cm)	Function
Orange	30	Sensor power to Arduino 5 Volt, splits into orange for parallel circuit
Gray	30	Sensor ground to Arduino ground
Green	30	Sensor output to Arduino input 0
Red	5	Servo power to Arduino 5 Volt, splits into orange for parallel circuit
Black	5	Servo ground to Arduino ground
Blue	5	Servo PWM to Arduino PWM 9
yellow	8	9 Volt battery to Arduino power supply

Table 5: Electrical circuitry involving servo motor, 9 Volt battery, Arduino and MyoWave Muscle Sensor.

Table 5).

Arduino

For this myoelectric prosthetic arm, the Arduino interpreted the sensor data from the MyoWare Muscle Sensor and activated the servo at the appropriate time to close or open the hand. The muscle sensor constantly sent sensor values to the Arduino. During a muscle contraction, the muscle sensor sent significantly higher values. The Arduino interpreted these higher values above a set threshold as a contraction of the muscle in the residual limb and triggered the servo to open or close the hand. The Arduino was powered by a 9-volt battery. The graph demonstrating the sensor values over time with

spikes exceeding the threshold during a muscle contraction is demonstrated in **(Figure 7)**.

Initially, each value of the sensor was intended to correspond to a different radian of the servo; much like a potentiometer works in the Arduino example servo code "knob." In this scenario, the fingers would be able to be gradually closed and opened by contracting the muscle a slight amount. When plugged into Arduino sensor example code "analog in out serial," the sensor revealed that during a muscle contraction, the user was unable to cause a gradual increase in sensor values by gradually contracting a muscle. Therefore, it was determined that a user could not control the fingers with enough accuracy using this code.

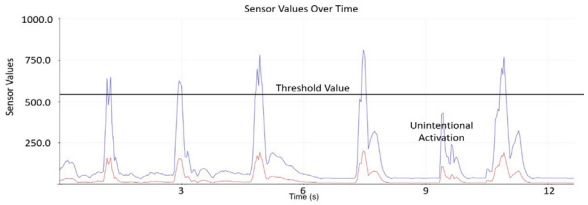

Figure 7: MyoWare Muscle Sensor values over time.

The second iteration relied on a threshold value. This simple code activated the servo to close the hand only when the sensor sent a sensor value over a certain number, which would indicate a muscle contraction. This provided satisfactory results; however, often even when at rest, the sensor sent values that suggested a muscle contraction despite the muscle being at rest. To combat this inaccuracy, a new code was made that averaged the values collected over 500 milliseconds. The average of these values was compared to the threshold value; if the average value exceeded the threshold value, the servo arm would turn and close the hand. This third version nullified almost all random unintentional activations of the servo. Though this code worked, the resting and flexing ranges vary from person to person. Therefore, calibration was required for each new user. Each unique threshold value was found by using a modified form of example code "analog in out serial," which graphed each user's resting and flexing values over time.

Servo

The servo used in this project is a 5-Volt servo motor. The fishing lines, or "tendons," were threaded through the fingers, palm, and forearm and attached to the arm of the servo, located on top of the servo. When activated, the servo arm rotated 180º to shorten the fishing line and close the fingers. To return the hand to its open position, the servo arm returned to its original position, releasing the fishing line, and the orthodontic bands pulled the fingers back into place. **(Figure 6, Table 5)**

Circuitry

The muscle sensor had a power, ground, and output wire. The sensor power and ground wires were connected to the Arduino's 5-Volt and ground ports respectively and were wired in parallel with the servo's power and ground ports. The sensor's output wire was joined to the Arduino's input 0 port. The servo had three wires: a power, a ground, and a Pulse-Width Modulation (PWM) wire. The servo's power and ground wires were attached to the Arduino's 5-Volt and ground ports, respectively. The servo PWM wire entered the Arduino PWM 9 port.

(Figure 6) demonstrates the electrical connections between the sensor, Arduino, servo, and 9-Volt battery. The color-coded lines and their corresponding electrical connections are reflected in **(Table 5).**

Vibrotactile Feedback

The vibrotactile feedback mechanism was independent from the Arduino circuit. It was a simple circuit that consists of a touch sensor, AAA battery, and vibrating motor from a mobile phone. The touch sensor was placed on the tip of the index finger of the prosthetic. When triggered, the touch sensor would allow the current to flow through the circuit and activate the vibrating motor attached to the residual limb via a plastic mount inside the forearm. The user would subsequently feel a vibrating sensation on the residual limb which would alert them that the prosthetic has come in contact with an object.

Testing of the Myoelectric Prosthetic Arm with Vibrotactile Feedback

The participant performed each task five times, blindfold and non-blindfolded, with and without vibrotactile feedback. Task efficiency was determined by the time it took in seconds for the tasks to be completed. Failure to complete a task is defined as taking longer than 60 seconds.

The paired sample t-test in Microsoft Excel was used to compare the statistical difference between the presence and absence of vibrotactile feedback in task performance while the participant was blindfolded and non-blindfolded.

Tests Comparing Time for the Blindfolded Participant to Perform 3 Functional Tests Using the 3D-Printed Myoelectric Prosthetic Arm with & without Vibrotactile Feedback

1) The participant was asked to determine if the index finger with the tactile sensor was being touched.
2) The participant was asked to determine if a plastic block was placed on the palm.
3) The participant had to locate a plastic block on the tray.

Tests Comparing Time for the Non-blindfolded Participant to Complete Eight Daily Tasks Using the 3D-Printed Myoelectric Prosthetic Arm with & without Vibrotactile Feedback.

1) Pick up a coin
2) Cut food

3) Pick up a light object (plastic block, 20g)
4) Pick up a heavy object (stapler, 500g)
5) Hold a cup
6) Pick up a bottle and transfer it onto a tray
7) Hold a tray
8) Squeeze toothpaste on the toothbrush

Received: April 30, 2019
Accepted: October 2, 2019
Published: November 25, 2019

REFERENCES

1. "Limb Loss Statistics". *Amputee-Coalition*, 2018. www.amputee-coalition.org/resources/limb-loss-statistics
2. "Cosmetic Upper Limb Prosthetics". *Ottobockus*, 2016. www.ottobockus.com/prosthetics/upper-limb-prosthetics/solutionoverviewcosmetic-solutions/ [Cosmetic Upper Limb]. (n.d.).
3. "Body Powered Prosthetics". *Ottobockus.com*, 2016. www.ottobockus.com/prosthetics/upper-limb-prosthetics/solution-overview/body powered-prosthetics/ [Body Powered Prosthetic].
4. Carey SL, Lura DJ, Highsmith MJ. "Differences in Myoelectric and Body Powered Upper-Limb Prostheses: Systematic Literature Review". *Journal of Rehabilitation Research & Development*. Vol 52, 2015: 247-262
5. "Body Powered Prosthetics". *Hanger Clinic*. 2016. www.hangerclinic.com/limb-loss/adult-upper-extremity/pages/Body-Powered-Prostheses.aspx
6. "MyoelectricProsthetics".2016.www.myoelectricprosthetics.com
7. Chadwell, Alix C, et al. "The Reality of Myoelectric Prostheses: Understanding What Makes these Devices Difficult for Some Users to Control". *Frontiers in Neurorobotics*. Vol 10 7, 2016.
8. Balciunas A, et al " Viability and Function of Myoelectric Prosthetics as Compared to passive, Body-Powered, and Electrically Powered Prosthetics". University of Pittsburgh, *Swanson School of Engineering*. 3/8/2019
9. "Prosthetic Arm Cost". *CostHelper,* 2018. www.health.costhelper.com/prosthetic-arms.html [Prosthetic Arm Cost]
10. Zhu H et al. "Dexterous Manipulation with Reinforcement Learning: Efficient, General, and Low Cost" B*erkeley Artificial Intelligence Research*. August 31, 2018. www.bair.berekely.edu/blog/2018/08/31/dexterous-manip/
11. Hobbs A. "Open Bionics' Releases Affordable 3D Printed Bionic Arm" *Internet of Business*. April 24, 2018. www.internetofbuisiness.com/open-bionics-hero-arm/
12. Nabeel, M et al. Vibrotactile Stimulation for 3D-Printed Prosthetic Hand. 2016 . *2nd International Conference on Robotics and Artificial Intelligence (ICRAI*). Nov 2, 2016.
13. Schiefer M et al. Sensory Feedback by Peripheral Nerve Stimulation Improves Task Performance in Individuals with Upper Limb Loss Using Myoelectric Prosthesis. *Journal of Neural Engineering*. Feb 13, 2016
14. Lawera N et al. Real-time Dextrous Fine Motor Control of an Advanced Prosthetic Arm Using Regenerative Peripheral Nerve Signals. *Plastic and Reconstructive Surgery.* April 2019-Vol 7
15. "3D-Printer Filament". *Matterhackers*. 2019. www.matterhackers.com/3d-printer-filament-compare [ABS Filament].

ACKNOWLEDGEMENTS

I would like to express my gratitude to Dr. Ha Vo for giving me the opportunity to travel to Vietnam with Mercer on Mission, which provided me the inspiration for this project. Many thanks to my participant for her time and patience during the task performance testing. Finally, a special thank you to Mr. Malmberg, my physics/robotics teacher and mentor for this project. His enthusiasm was infectious, and his ongoing support gave me the encouragement to see this research to its completion.

JOURNAL OF
EMERGING INVESTIGATORS

Article

Anonymity reduces generosity in high school students

Elton Emiliano Vargas-Guerrero, Jorge Armando Grajales-Rodríguez, and María Elena Cano-Ruiz
Tecnologico de Monterrey, Cuernavaca High School, Mexico

SUMMARY

The disinterested willingness a person has for helping others is known as altruism. But is this willingness to help others dependent on external factors that make you more or less inclined to be generous? We hypothesized that generosity in adolescents would depend on external factors and that these factors would change the amount of help given. To evaluate altruism and generosity, we conducted non-anonymous and anonymous variations of the dictator game and ultimatum game experiments and explored the role of anonymity, fairness, and reciprocity in high school students. Instead of using money, we randomly selected high school students from six science classrooms to receive extra points on their midterm exam, while the rest of the students did not receive extra points. The students that received extra points became donors, while the students that did not receive extra points became recipients. We varied the ability to redistribute points in three ways. One, donors could donate points, showing true altruism. Two, donors could donate or steal points from the recipients, allowing us to assess fairness. Finally, donors could donate points, but the allocation of points depended upon recipients accepting or rejecting the proposed donation in a measure of fairness and reciprocity. We found that both anonymity and the possibility of taking points decreased the willingness to give, while reciprocity increased the willingness to give as the students based their decision more on strategy than generosity. We concluded that generosity in adolescents is mostly dependent on personal gain and peer judgment rather than pure altruism.

INTRODUCTION

Throughout human history, there has been uncertainty about the factors that determine the disinterested willingness a person has for helping others, and no easy answer has been found. There are two main lines of thought outlining proposed reasons why humans help others: the line of egoism and the line of altruism (1). Supporters of the egoism line claim that deep down, everything people do has an ultimate goal of self-benefit, no matter how beneficial to others a decision may seem. By contrast, advocates of altruism claim that the ultimate goal is maximizing the well-being of others, and that self-benefit could be an indirect result when helping others (1). Prosocial behavior during which humans give to others can also be differentiated based on motivation. Pure altruistic behavior refers to unconditional giving and helping, norm-based behavior relates to fairness and punishment, and strategic prosocial behavior means giving only because the other can punish you (2). Additionally, feeling empathy motivates people to be altruistic, indicating that genuine concern for others can be part of human nature (2). Altruism is not plain self-sacrifice but rather the willingness to act considering the interests and conditions of others without considering any external motive (3). External motives can exist along with altruism, but they cannot be the only ones (4). One of the main motives of performing altruistic actions can be the personal benefit one gains for the simple act of giving without expecting anything in return (5).

In behavioral economics, a popular experiment used to test the roles of altruism, fairness, and self-interest is the dictator game, which captures the decision of a donor to allocate money to another or not and how much money is donated (6). Dictator games have been made throughout the world, and people have been found to give an average of twenty percent of what they were given (7, 8). Dictator experiments with children found an average of 29% of their participants gave their incentives away, concluding that children behave similarly to adults in these experiments because both live in social environments with continuous interactions that punish or reward their behavior (9).

When dictatorship games were created, they were initially managed to cut factors such as rewarding generosity and punishment of selfishness since recipients were anonymous and they did not have the power to do something about the donation (10). Variations of these games have been carried out, and they have been used to demonstrate that giving changes depending on the setting and specific conditions (10). In one variation of the classical dictator game, when the possibility of taking money exists, the average amount of money given decreases from 20% to zero. Simultaneously, the most selfish outcome is often not chosen, and most people do not take money from others (10). In another variation, when people are asked to work before giving money for donation, the amount of donations also decreases (10). Variations in how money is given to donors seem to cause changes in the perception of moral costs for donors, thus people tend to give less if they feel they earned the money by earlier work. Another game used in behavioral economics is the ultimatum game. During this game, the donor is tasked with splitting the given money with the recipient, but the recipient may accept

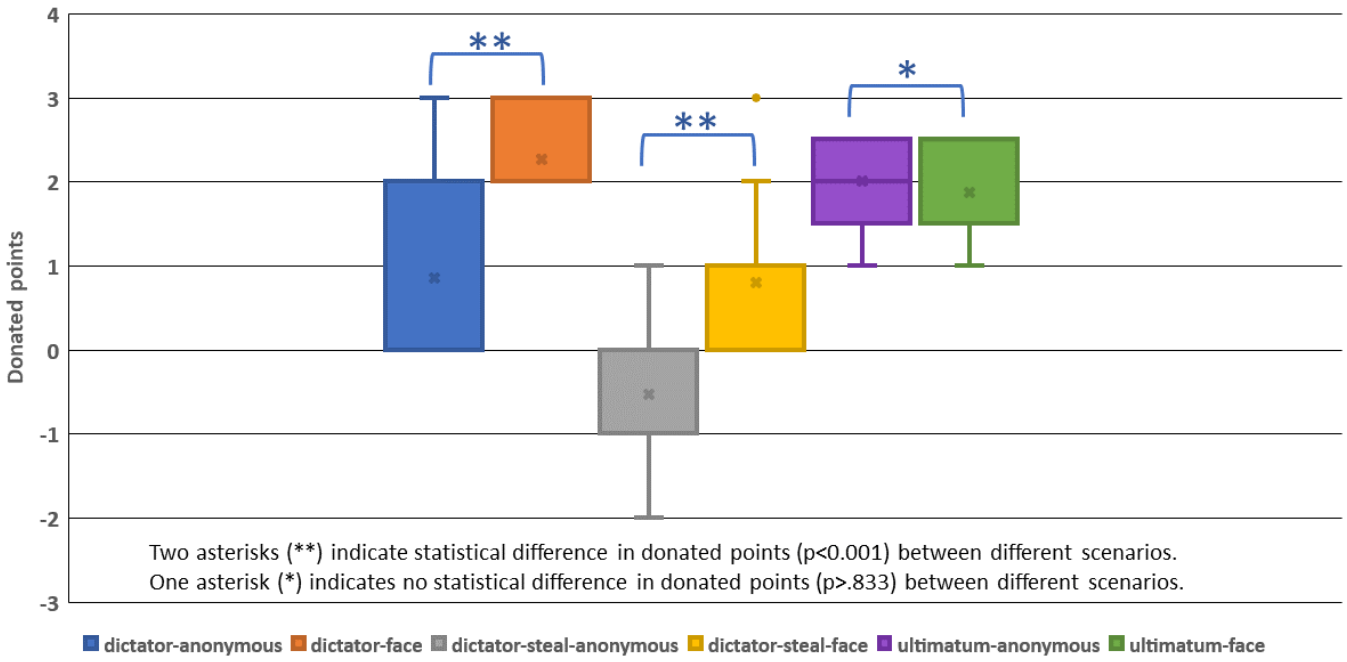

Figure 1. Points donated under two conditions. Dictator game: donors could donate from 0 to 5 points in anonymous (blue) or face-to-face donations (orange). Dictator-steal game: donors could donate from -2 to 3 points in anonymous (grey) or face-to-face donations (yellow). Ultimatum game: donors could donate between 0 and 5 points, and the outcome was dependent on the acceptance or rejection by the recipient in anonymous (purple) or face-to-face donations (green). There was a statistical difference in points donated in the dictator game between anonymous and face-to-face donations (**p-value = 0.0012), and in dictator-steal games between anonymous and face-to-face donations (**p-value = 0.0005). There was no statistical difference in points donated in ultimatum games between anonymous and faced-to-face donations (*p-value = 0.8331).

or reject the donation, and if the recipient rejects the donation, both players receive nothing (11). Therefore, the ultimatum game can be used to assess fairness and reciprocity between players.

We decided to explore the role of anonymity, fairness, and reciprocity in prosocial behavior of high school students using a variation of the dictator game, where extra points on the midterm test were allocated instead of giving money to students. We hypothesized that generosity in teenagers is conditioned upon external circumstances as well as personal gain. Therefore, we hypothesized that anonymity and personal gain would decrease the willingness of donors to give points to others.

RESULTS

To complete the experiment, we selected six science high school classrooms in Tecnologico de Monterrey High School, Mexico. The participants included 164 students (males and females) whose ages ranged from sixteen to nineteen years old. The students within each classroom were divided randomly into two groups. In three of the science classrooms, the members of these two groups interacted with each other in person (in a face-to-face interaction) to exchange the real extra exam points in the midterm test. In the other three classrooms, the exchange of real extra exam points was done anonymously. We varied the way donations of points were done in three ways. In the first variation, donors received 5/100 extra points (i.e. 5 extra points on a test scored out of a total of 100 possible points), and they were able to donate from 0 - 5 points (group dictator-anonymous and group dictator-face). In the second possible scenario, the donors received 3/100 extra points and could either choose to donate 0 - 3 points or steal 0 - 2 points from the recipients that also received 2/100 extra points (group dictator-steal-anonymous and group dictator-steal-face). In the third set up, donors received 10/100 extra points and could donate from 0 - 10 points, but the recipients could either accept or reject the proposed donation. If the recipients rejected the donation, extra points were not allocated to either the donors or recipients (group ultimatum -anonymous and group ultimatum-face).

The ability to allocate different amounts of total points for donors in the three different settings was as follows. For dictator and dictator-steal scenarios, the allocation of points was done so that the most points a person could get was five points in each scenario. For the ultimatum groups, a total of ten points were allocated for better determination of generosity, fairness, and reciprocity by having more options for the splitting of points.

For the analysis of variance (ANOVA) statistical analysis, the points of the three scenarios of donations were standardized to a range from zero to five. Statistical analysis using two-way ANOVA, one factor being anonymous or face condition and the other factor being the type of dictator game variation (dictator, dictator-steal, or ultimatum) indicated a

	Dictator	Dictator-steal	Ultimatum
Anonymous	17%	-11%	40%
Face-to-face (non-anonymous)	45%	16%	37%
Difference	28%	27%	-3%

Table 1. Mean percentages of points donated under the different conditions. The generosity of students increased for face-to-face donations in dictator and dictator-steal games but did not change in the ultimatum game.

statistically significant interaction between the two factors (anonymity vs. donation scenarios: p-value = 0.0003). The points donated decreased in anonymous conditions for dictator and dictator-steal treatments, but in the ultimatum game, the condition of anonymity did not affect the donation (**Figure 1**).

We compared the average number of points donated under different conditions (**Figure 1**). The spread of results of points donated in each classroom can be seen on the box plots. In the dictator scenario classrooms, the average number of points donated ± the standard deviation was 0.85 ± 1.21 points for the dictator-anonymous scenarios and 2.27 ± 0.89 points for the dictator-face scenarios (individual values ranging from 0 to 5). In the dictator-steal classrooms, the average was -0.53 ± 0.99 points for the dictator-steal anonymous scenarios and 0.8 ± 0.86 points for the dictator-steal-face scenarios (individual values ranging from -2 to 3). In the ultimatum classrooms, the average was 2 ± 0.33 points for the ultimatum-anonymous scenarios and 1.86 ± 0.40 points for the ultimatum-face scenarios (values standardized ranging from 0 to 5) (in **Figure 1**, means are marked with an x).

We calculated the significance of the difference between the anonymous and face-to-face conditions for each variation of the dictator and ultimatum games using t-tests for two independent samples (**Figure 1**). We found a statistically significant difference between the mean number of points donated in anonymous and face-to-face dictator games (p-value = 0.0012). Similarly, we found a statistically significant difference between the mean number of points donated in dictator-steal games with and without anonymity (p-value = 0.0005). But we found no statistically significant difference in the mean number of points donated between the anonymous and face-to-face ultimatum conditions (p-value = 0.5909).

The mean percentages of points donated under the different conditions show the generosity of the students (**Table 1**). When we compared the anonymous conditions and face-to-face conditions between dictator and dictator-steal games, we found a similar trend. Face-to-face conditions increased the number of points donated (**Figure 1**). In both game types, there was a 27-28% difference in the percentage of points donated when the groups interacted face to face instead of anonymously. However, in the ultimatum game, the difference between anonymous and face-to-face donations was not important (3%) and around 40% of the points were donated, similar to face-to-face dictator game (45% donated points). Comparing dictator vs. dictator steal settings, donors in the dictator steal group decreased the number of points they gave away, regardless of whether the conditions were anonymous or face to face (**Figure 1**).

DISCUSSION

Different studies where dictator games were made throughout the world found that people gave on average twenty percent of what they were given under anonymity (7,8,10), which could be considered as altruistic behavior. Nevertheless, varying the set of action choices and the origin of the endowment gives different results (10). Taking this into account, the results of our experiments with 17% of points donated on average under anonymous dictator game (**Table 1**) were not as different as the average 20% donation of money found in previous research (7,8,10) considering that regardless of the conditions, on average people did give a part of what was given to them. If we consider only this result, we may be led to conclude that people are naturally altruistic because they tend to donate. However, other important factors need analysis because we conducted dictatorship games with extra exam points under different conditions (**Figure 1**, **Table 1**). When the conditions of the dictatorship games changed, donations from the dictators suffered significant changes, and when donors could take money from the recipient, donations reduced, and some donors even took money from recipients (10).

In our experiments, the results followed the same pattern as mentioned above. We were also able to see that donations reduced in response to anonymity (**Figure 1**), as well as in the dictator-face group allowed only to donate to recipients (mean of 45% points donated) compared to the dictator-steal-face group that could either give or take away points from the recipient (mean of 16% points donated). There are likely two reasons donors donated fewer points in the dictator-steal scenarios. First, since recipients received two extra points in the dictator-steal scenario, donors presumably concluded that a fair condition was already established. Second, donors had the opportunity to steal points, which decreased the moral cost for donors. The donors likely felt that it was fair not to donate points because they were turning down the option to steal from others, even in non-anonymous conditions. We conclude that when given a situation of fairness (each party gains points from the beginning), students are less likely to be altruistic.

Under the ultimatum game, in which the allocation of points for the donor and recipient was dependent on acceptance by the recipient, donors were as generous as under the dictator game face to face (45% donation), regardless of whether the ultimatum game was anonymous (40% donation) or face-to-face (37% donation). This indicates that the donations in

these cases may be driven by strategy and the donors' fear of losing their points if they do not give fairly.

We varied the conditions of the dictatorship games to explore the effect of anonymity on altruism. Social behavior can be explained by purely external causes and a significant part of such behavior is influenced by social norms (12). Moreover, when carrying out non-anonymous dictatorship games, there was a significant increase in donations when these donations were to a person thought to be "deserving" (13). In our face-to-face dictator-steal and ultimatum games, norm-based prosocial behavior and strategic prosocial behavior were responsible for the donation of points, resulting in a decrease in the number of points donated compared to the original dictator-game due to a reduction in moral cost and increase in moral disengagement (10, 14). Moral disengagement in adolescents temporarily allows them to ignore moral responsibilities towards others (14). This enables them to prioritize their own needs over those of others (14). Nevertheless, the mean donation of points in the dictator game and the dictator-steal game increased significantly from anonymous to face-to-face (non-anonymous), indicating a strong influence of peer judgment and the presence of social norm motivation and prosocial behavior on the donation outcome (**Table 1**). The importance of peer influence in teenagers has been related to neural brain processes in the developing adolescent brain. Peer influence evokes activation in the social brain network, influencing teenagers on prosocial decision making (15, 16). This social brain network activation occurs much less in children or adults (15, 16).

On the other hand, in the ultimatum scenario, when the allocation of points for both donor and recipient was dependent on the acceptance or rejection of the recipient, anonymity had no impact on the outcome. Although some generosity could be observed, strategic prosocial behavior dependent on giving only because the other can inflict punishment seems more probable (2). Under the ultimatum game, which was trying to check fairness and reciprocity, the lowest offer was 1 out of 5 points (2 out of 10 in non-standard values), and the donor kept 4 of 5 points (8 out of 10 in non-standard values). No recipient rejected the offered donation, even if a small donation seemed unfair. This could be because it is more convenient to end up gaining a little, even if the circumstances are not ideal.

Comparing results among the different scenarios, we conclude that students were not purely altruistic. Instead, they let external factors influence their giving. We found that more points are donated in non-anonymous environments compared to anonymous conditions. Furthermore, when altruism was evaluated with fairness added, most of the students did not give points to the recipients. This may have been because the recipients already had gained points. In some instances, students even took points from the recipient in anonymous conditions for personal gain. When the donations of points were evaluated with fairness and reciprocity added, students on average split the points given. They acknowledged that if the recipient did not like the proposed donation, both would have lost the points, independent of the presence or absence of anonymity.

To further gain understanding about generosity and altruism among adolescents, this study can be expanded by considering other factors, such as evaluating if the recipient's need for points could trigger empathy in the donors and increase donations. To accomplish this test, one could create scenarios where the recipients are students that need extra points. Another variation of the test could be to have the donors be students that do or do not need extra points. These results would clarify the extent to which students would relate and respond to a perceived need in others. Our results are important because they show us that social behavior can be influenced by external forces, supporting our hypothesis that generosity in adolescents is dependent upon external circumstances as well as personal gain.

METHODS

The experiments were performed at the Tecnologico de Monterrey-Cuernavaca high school, Mexico. Participants included six science classrooms with a total of 164 students (46% males and 54% females). Student ages ranged from sixteen to nineteen years old. The members of each classroom were divided randomly into two groups. In three of the science classrooms, the two groups interacted face-to-face in an exchange of real extra exam points on the midterm test between their members. In the other three classrooms, the exchange of extra exam points was done anonymously. In all the groups, talking was forbidden during the experiment to avoid negotiations in the exchange of points. The extra points were given one week before the midterm tests, so the midterm score would not affect the donations.

Every classroom was presented with different conditions for exchanging the extra points. Four same level Chemistry course classrooms (11th grade students, n = 26 for group 1 and n = 30 for groups 2, 3, and 4) and two same level Introduction to Research Method course classrooms (12th grade students, n = 26 for group 1 and n = 22 for group 2) participated in this study. Members of the chemistry classroom 1 (dictator-anonymous) were told that their teacher gave half of the group (donors) five out of one hundred points on their midterm exam and gave the other half (recipients) no points. Then, students randomly were given a piece of paper to indicate if they were donors or recipients. It was also explained that the students who received the points had the opportunity to decide and write on that piece of paper if they wanted to donate from zero to five extra exam points to another anonymous classmate chosen randomly that did not receive the points. Students that did not receive any points were just asked to write their names on the paper given to them. Finally, they were told that matches between donors and recipients were going to be done randomly and the number of points each student ended with was going to be communicated after the midterm exam was taken by all students, the next week.

In the chemistry classroom 2 (dictator-face), the procedure was the same as in chemistry classroom 1 (dictator-anonymous); however, in chemistry classroom 2, pairs of students were matched randomly at the beginning and a face-to-face, non-anonymous condition was placed. Students were told that one member of the pair was going to receive the points (donor) and the other one was not (recipient). They were given a piece of paper randomly that indicated if they were the donors or the recipients, and they were asked to write their name, their donation decision, and the name of their partner. Recipients were just asked to write their name and the name of their partner. After the experiment, they were told that results were going to be communicated after the midterm exam was taken by all students the following week.

Students of chemistry classrooms 3 and 4 (dictator-steal-anonymous and dictator-steal-face) were told that half of the classroom (donors) received three out of one hundred points in the midterm exam and the other half (recipients) received two exam points. Group members that received three exam points were told that they had the opportunity to either donate zero to three points or take away zero to two points from one of their classmates (recipients). The rules for assigning donors and recipients randomly and the anonymous or face-to-face non-anonymous conditions were the same as described above, with chemistry classroom 3 working on anonymous conditions and chemistry classroom 4 under face-to-face non-anonymous conditions.

Two more experiments were done in the research methods classrooms. In research methods classroom 1 (ultimatum-anonymous), students were randomly divided in two groups, and then students were told that one group (donors) would receive ten out of one hundred points in the midterm exam and that the other group (recipients) would not receive any points. Papers that indicated if you received the points or not were randomly assigned to every student, and students that received the points were asked to write on the papers if they wanted to donate from zero to ten extra exam points to other student that did not received any points. Before writing down their decisions, students were told that the anonymous recipient had the decision of accepting or rejecting the donation, but if the recipient rejected the donation, no one received any extra exam points. Each of the donor and recipient papers had one three-digit identification number so that every donor could be matched with the recipient that had the same identification number. After every donor wrote his or her decision, papers were collected, and donors were asked to leave the classroom for the purpose of conserving anonymity. After donors left the class, recipients received the proposed donation and wrote down whether they accepted or rejected the offer. Donation decisions were communicated to recipients according to their identification number.

In research methods classroom 2 (ultimatum-face), student pairs were assigned randomly (as in non-anonymous chemistry courses) and then students were told that one member (donor) of the pair would receive ten out of one hundred points on the midterm exam and that the other person (recipient) would not receive any points. The papers that indicated whether you receive the points or not were randomly assigned to every student, and students that received the points were asked to write on the papers if they wanted to donate from zero to ten exam points to his or her partner. Before writing down their decisions, students were told that his or her partner had the right to either accept the donation so that both received the extra exam points allocated or reject it so that no one received any extra exam points. After donors wrote their decisions, they passed the paper to the recipient. Recipients needed to write on their paper whether they accepted or rejected the donation, and the decisions were communicated to the donors.

The decision to allocate different amounts of total points for donors in the different settings was as follows: for dictator and dictator-steal scenarios, the most points a person could get was 5 points in each scenario. For the ultimatum groups, a total of 10 points were allocated for better determination of generosity, fairness, and reciprocity since there are more options for splitting points. For the statistical analysis, the points of the three scenarios were standardized in a range from 0 to 5 (dictator scenarios remained the same from 0 to 5, dictator-steal values were standardized adding 2 points: so went from -2 to 3 to 0 to 5, and ultimatum scenario were standardized dividing the values by 2, so went from 0 to 10 to 0 to 5).

Statistical Analysis

The data were analyzed using two-way ANOVA in a 2x3 factorial design, with one factor having two levels: anonymity and non-anonymity, and the other factor having three levels: dictator, dictator-steal, and ultimatum scenarios. After standardizing the values for the three different scenarios and since the sample sizes were not balanced, for the two-way ANOVA (with Microsoft Office Excel Data Analysis Tool pack, 2016), the missing cells for each sample were filled using the weighted means for each treatment to have the same sample size for each treatment (17).

After ANOVA showed significant interaction, t-tests for two independent samples assuming unequal variances (Microsoft Office Excel Data Analysis Tool pack, 2016) were done to compare each pair of classrooms that followed the same procedure with the only difference of anonymity or no anonymity (face-to-face). The significance threshold was set at $p = 0.05$.

ACKNOWLEDGMENTS

The authors would like to thank teacher Lilia Villalba-Almendra for allowing us to use her high school chemistry groups as participants and for donating extra points to her students in their midterm test for carrying out these experiments.

REFERENCES

1. Batson, C. Daniel, and Laura L. Shaw. “Evidence for Altruism: Toward a Pluralism of Prosocial Motives.” Psychological Inquiry, vol. 2, no. 2, 1991, pp. 107–122., doi:10.1207/s15327965pli0202_1.
2. Böckler, Anne, et al. “The Structure of Human Prosociality.” Social Psychological and Personality Science, vol. 7, no. 6, Aug. 2016, pp. 530–541., doi:10.1177/1948550616639650.
3. Gert, Bernard, and Thomas Nagel. “The Possibility of Altruism.” The Journal of Philosophy, vol. 69, no. 12, 1972, p. 340., doi:10.2307/2024778.
4. Andreoni, James, et al. Altruism in Experiments. New Palgrave Dictionary of Economics, 2nd Ed, 2007, https://econweb.ucsd.edu/~jandreon/Publications/PalgraveAltruism.pdf.
5. Andreoni, James. “Impure Altruism and Donations to Public Goods: A Theory of Warm-Glow Giving.” The Economic Journal, vol. 100, no. 401, 1990, p. 464., doi:10.2307/2234133.
6. “Dictator Game.” Wikipedia, Wikimedia Foundation, 2 Sept. 2019, https://en.wikipedia.org/wiki/Dictator_game.
7. Kahneman, Daniel, et al. “Fairness as a Constraint on Profit Seeking: Entitlements in the Market.” Choices, Values, and Frames, 2000, pp. 317–334., doi:10.1017/cbo9780511803475.019.
8. Forsythe, Robert, et al. “Fairness in Simple Bargaining Experiments.” Games and Economic Behavior, vol. 6, no. 3, 1994, pp. 347–369., doi:10.1006/game.1994.1021.
9. Harbaugh, W. “Childrens Altruism in Public Good and Dictator Experiments.” Economic Inquiry, vol. 38, no. 1, Jan. 2000, pp. 95–109., doi:10.1093/ei/38.1.95.
10. List, John A. “On the Interpretation of Giving in Dictator Games.” Journal of Political Economy, vol. 115, no. 3, 2007, pp. 482–493., doi:10.1086/519249.
11. “Ultimatum Game.” Wikipedia, Wikimedia Foundation, 6 Sept. 2019, https://en.wikipedia.org/wiki/Ultimatum_game.
12. Koch, Alexander and Hans Theo Normann. "Giving in dictator games: regard for others or regard by others?". Southern Economic Journal. 2008, 75(1). 223-231. https://EconPapers.repec.org/RePEc:sej:ancoec:v:75:1:y:2008:p:223-231
13. Eckel, Catherine C., and Philip J. Grossman. “Altruism in Anonymous Dictator Games.” Games and Economic Behavior, vol. 16, no. 2, 1996, pp. 181–191., doi:10.1006/game.1996.0081.
14. Paciello, Marinella, et al. “Moral Dilemma in Adolescence: The Role of Values, Prosocial Moral Reasoning and Moral Disengagement in Helping Decision Making.” European Journal of Developmental Psychology, vol. 10, no. 2, 2013, pp. 190–205., doi:10.1080/17405629.2012.759099.
15. Somerville, Leah H., et al. “A Time of Change: Behavioral and Neural Correlates of Adolescent Sensitivity to Appetitive and Aversive Environmental Cues.” Brain and Cognition, vol. 72, no. 1, 2010, pp. 124–133., doi:10.1016/j.bandc.2009.07.003.
16. Hoorn, Jorien Van, et al. “Peer Influence Effects on Risk-Taking and Prosocial Decision-Making in Adolescence: Insights from Neuroimaging Studies.” Current Opinion in Behavioral Sciences, vol. 10, 2016, pp. 59–64., doi:10.1016/j.cobeha.2016.05.007.
17. R Tutorial Series: Two-Way ANOVA with Unequal Sample Sizes ... https://www.r-bloggers.com/r-tutorial-series-two-way-anova-with-unequal-sample-sizes/.

Article submitted: April 10, 2019
Article accepted: June 5, 2019
Article published: November 25, 2019

Sponsorship

Editor's Circle $10,000+

ALLOY THERAPEUTICS

Patron $5,000+

NEW ENGLAND BioLabs® Inc.
enabling technologies in the life sciences

PORTFOLIOS WITH PURPOSE®

Institutional Supporters

HARVARD UNIVERSITY

HARVARD MEDICAL SCHOOL

Tufts UNIVERSITY

Charitable Contributions

We need your help to provide mentorship to young scientists everywhere.

JEI is supported by an entirely volunteer staff, and over 90% of our funds go towards providing educational experiences for students. Our costs include manuscript management fees, web hosting, creation of STEM education resources for teachers, and local outreach programs at our affiliate universities. We provide these services to students and teachers entirely free of any cost, and rely on generous benefactors to support our programs.

A donation of $30 will sponsor one student's scientific mentorship, peer review and publication, a six month scientific experience that in one student's words, 're-energized my curiosity towards science', and 'gave me confidence that I could take an idea I had and turn it into something that I could put out into the world'. **If you would like to donate to JEI, please visit https://emerginginvestigators.org/support, or contact us at questions@emerginginvestigators.org.** Thank you for supporting the next generation of scientists!

'Journal of Emerging Investigators, Inc. is a Section 501(c)(3) public charity organization (EIN: 45-2206379). Your donation to JEI is tax-deductible. '

emerginginvestigators.org